



**The Abdus Salam
International Centre for Theoretical Physics**



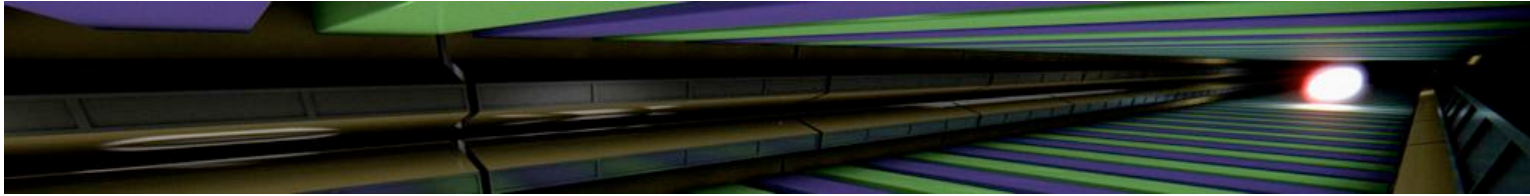
2139-2

**School on Synchrotron and Free-Electron-Laser Sources and their
Multidisciplinary Applications**

26 April - 7 May, 2010

Scientific Use of Hard X-ray Free-Electron Lasers

Massimo Altarelli
*European X-ray Free-Electron Laser Facility
Hamburg*



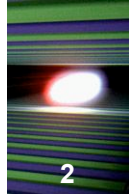
Scientific Use of Hard X-ray Free-Electron Lasers

Massimo Altarelli

*European X-ray Free-Electron Laser Facility
22607 Hamburg, Germany*

www.xfel.eu for more information....

Third Generation Synchrotron Sources



Diamond, Didcot, UK



ESRF, Grenoble, France



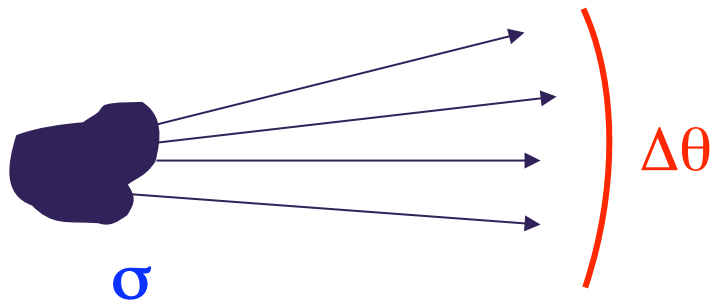
PETRA III, Hamburg, Germany





FLUX OF PHOTONS IN UNIT SPECTRAL RANGE (SOURCE AREA) X (BEAM DIVERGENCE)

Units: photons/s/mm²/mrad²/0.1%BW



$$B = \frac{\Phi}{\sigma \Delta\theta_h \Delta\theta}$$



2003 Roderick McKinnon
Structure of Cellular Ion Channels

1997 John E. Walker
Structure of F1-ATPase



2006 Roger D. Kronberg
Structure of RNA polimerase



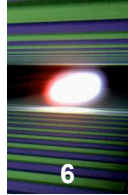
3 Win Nobel for Ribosome Research



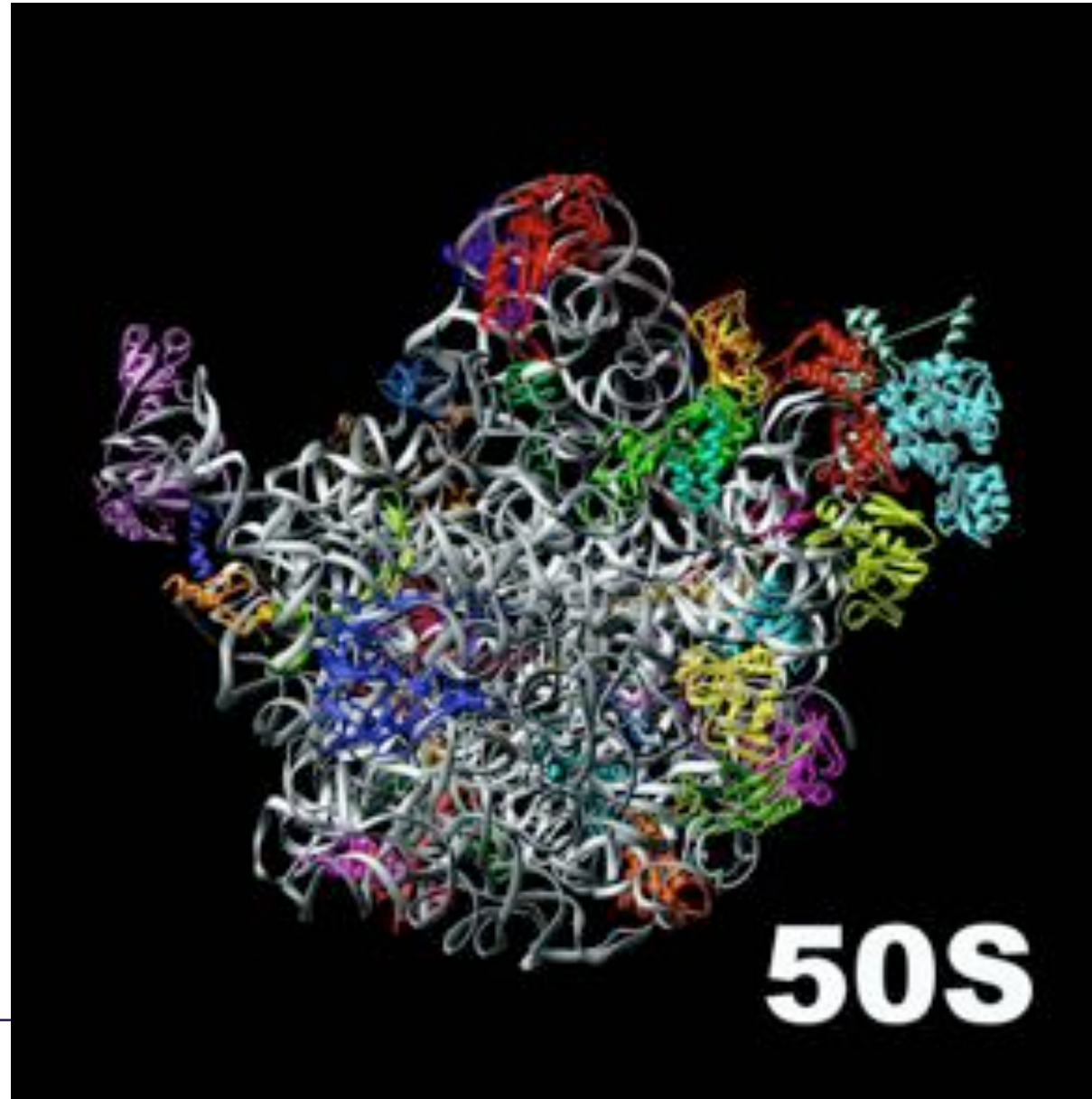
Reuters

From left, Venkatraman Ramakrishnan of the MRC Laboratory of Molecular Biology in Cambridge, England; Thomas A. Steitz of Yale University; and Ada E. Yonath of the Weizmann Institute of Science in Rehovot, Israel, will share the 2009 Nobel Prize in Chemistry.

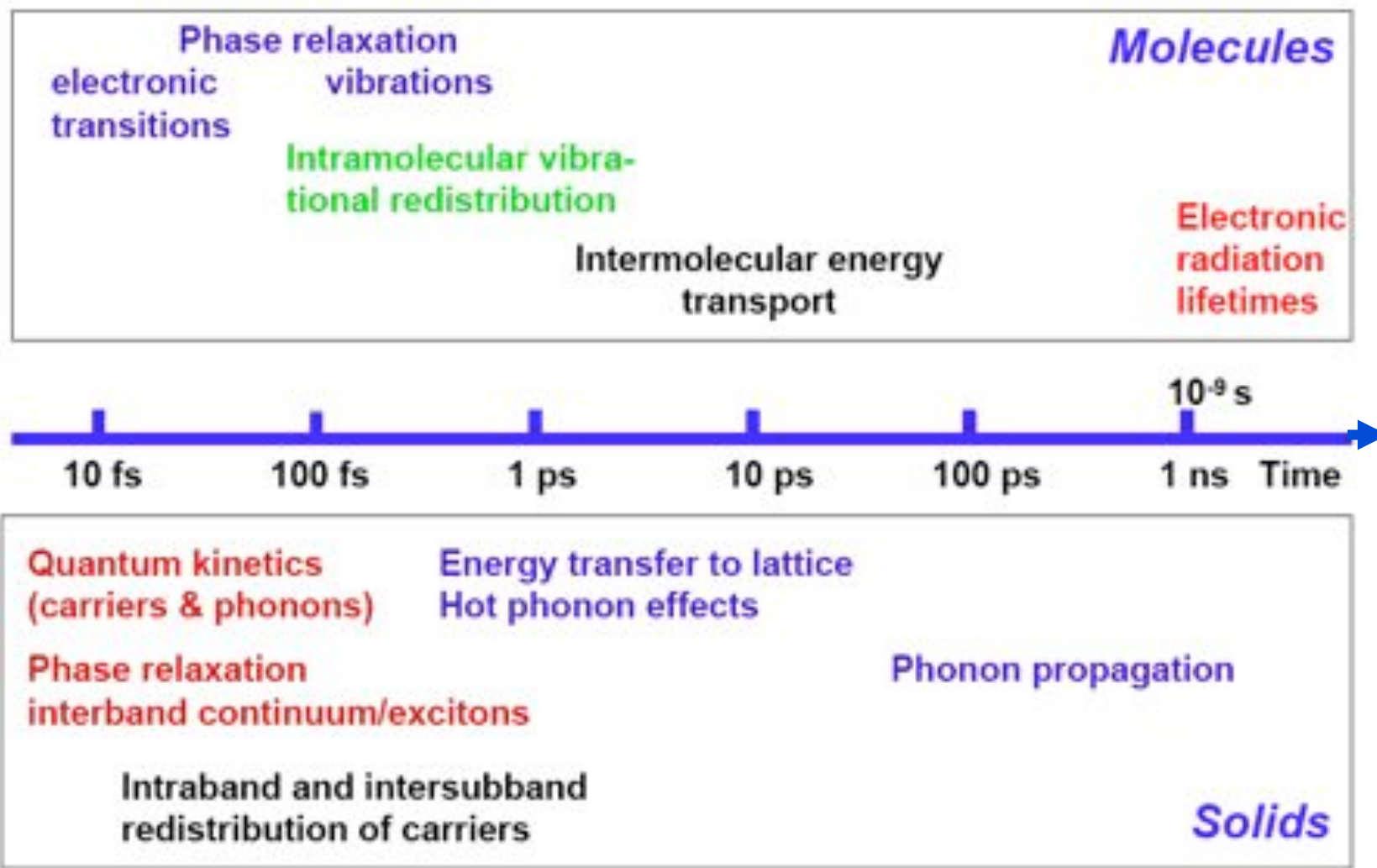
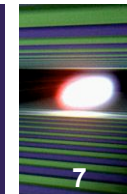
Working independently and using, among other things, the X-rays generated by powerful particle accelerators and prodigious computer calculations, the three winners and their colleagues succeeded in mapping the locations of the hundreds of thousands of atoms in the giant molecular complexes . . .

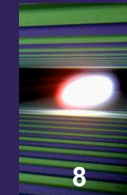


From the home
page of Ada
Yonath



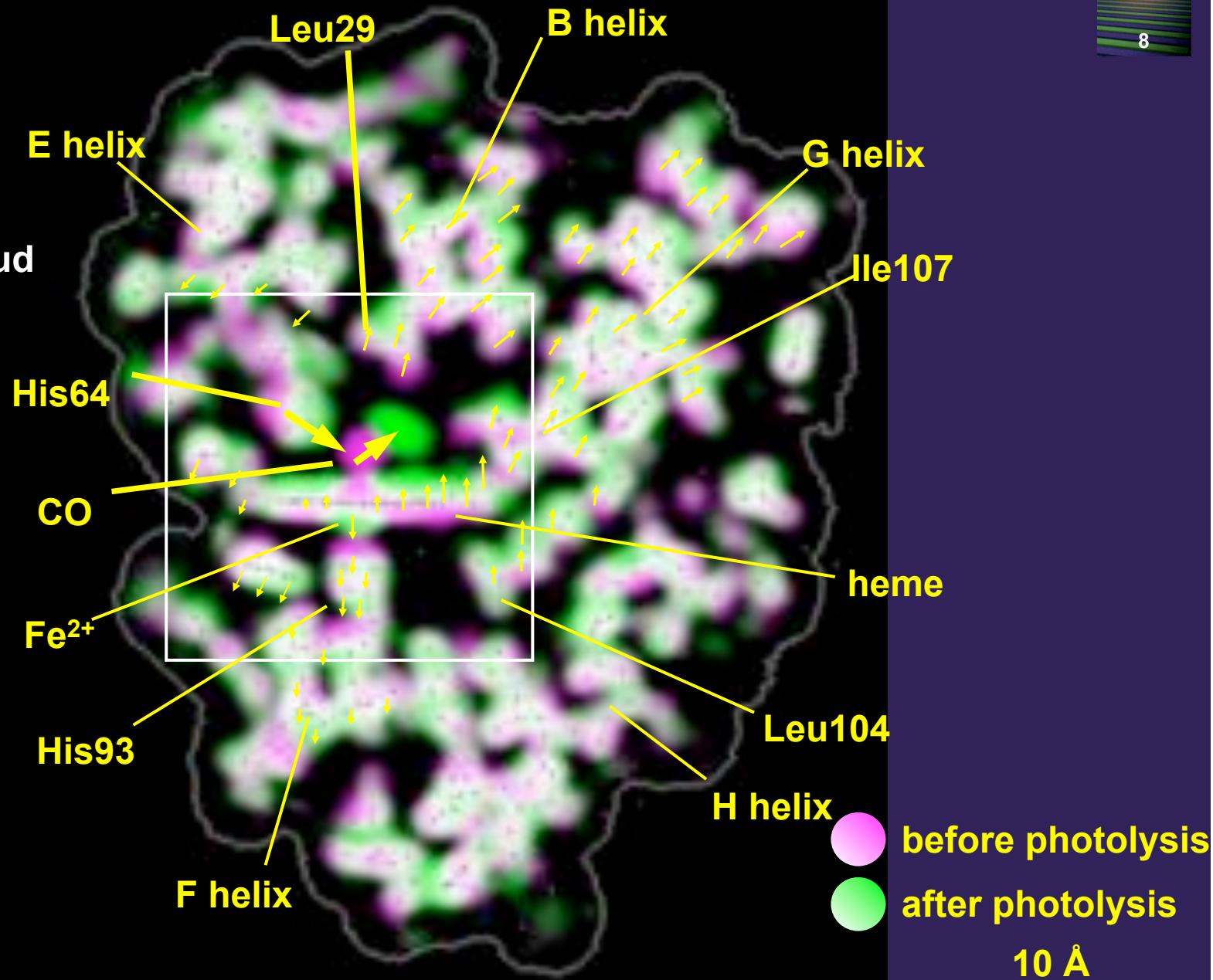
Time Scales for Dynamics



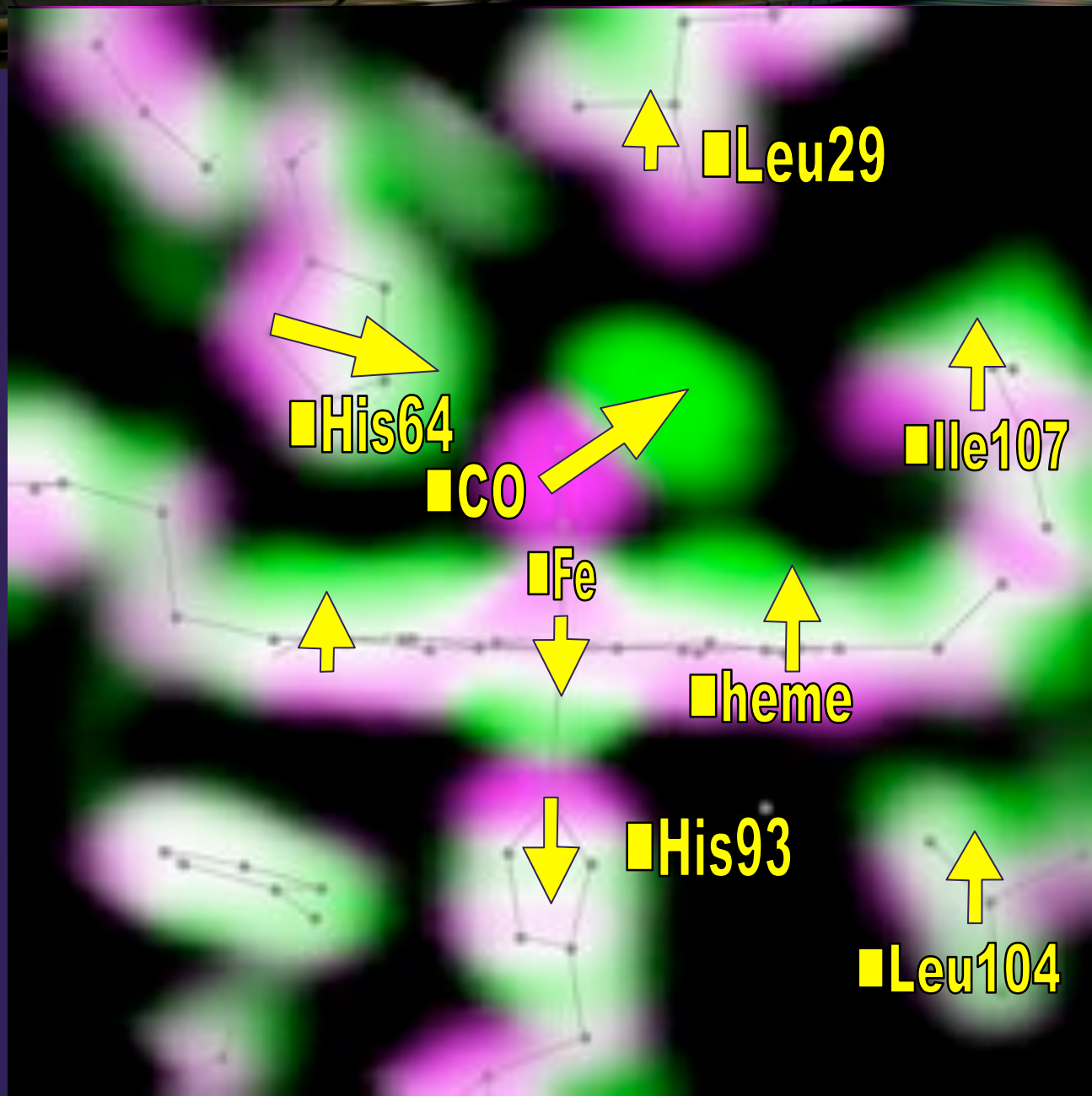


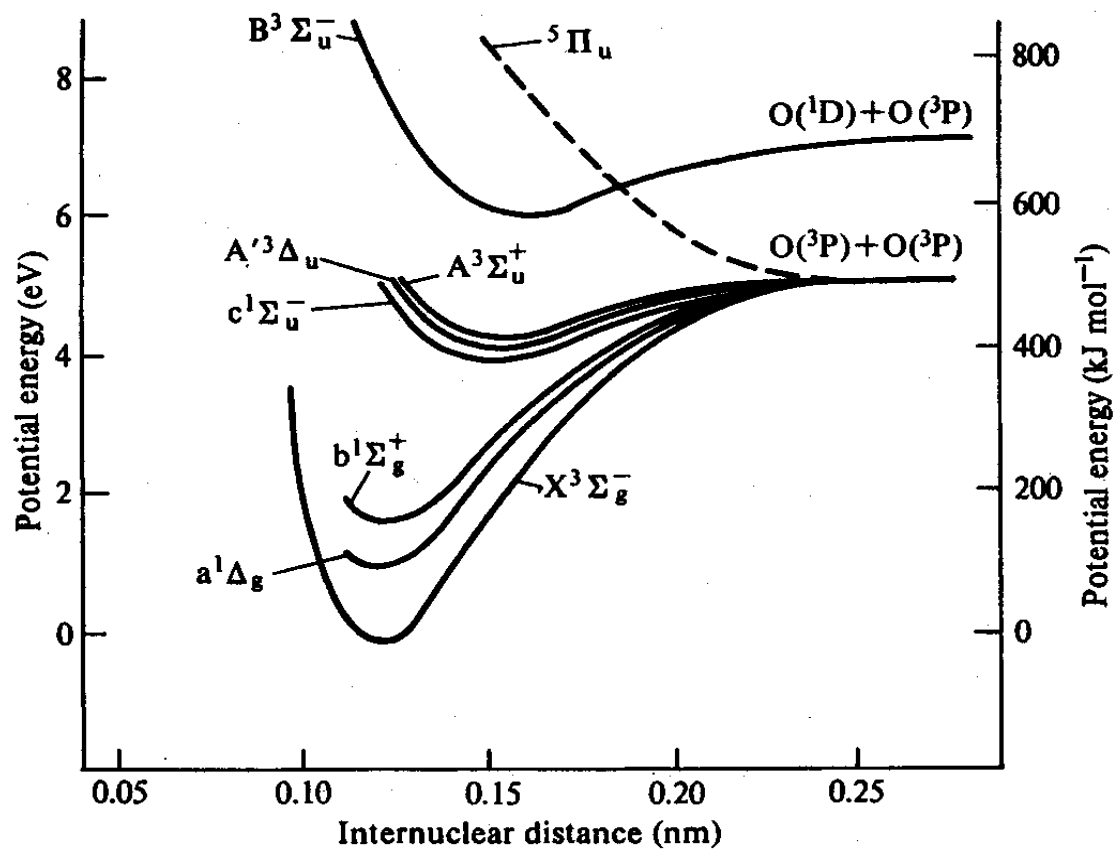
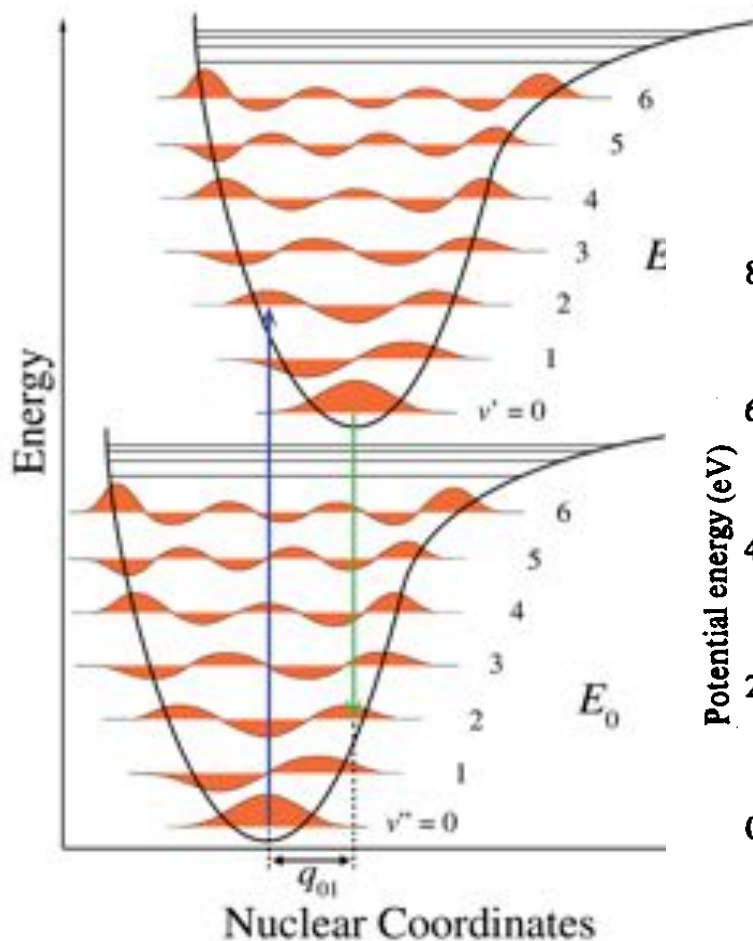
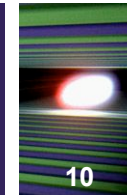
After Ph. Afinrud

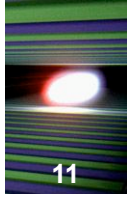
ESRF ID09



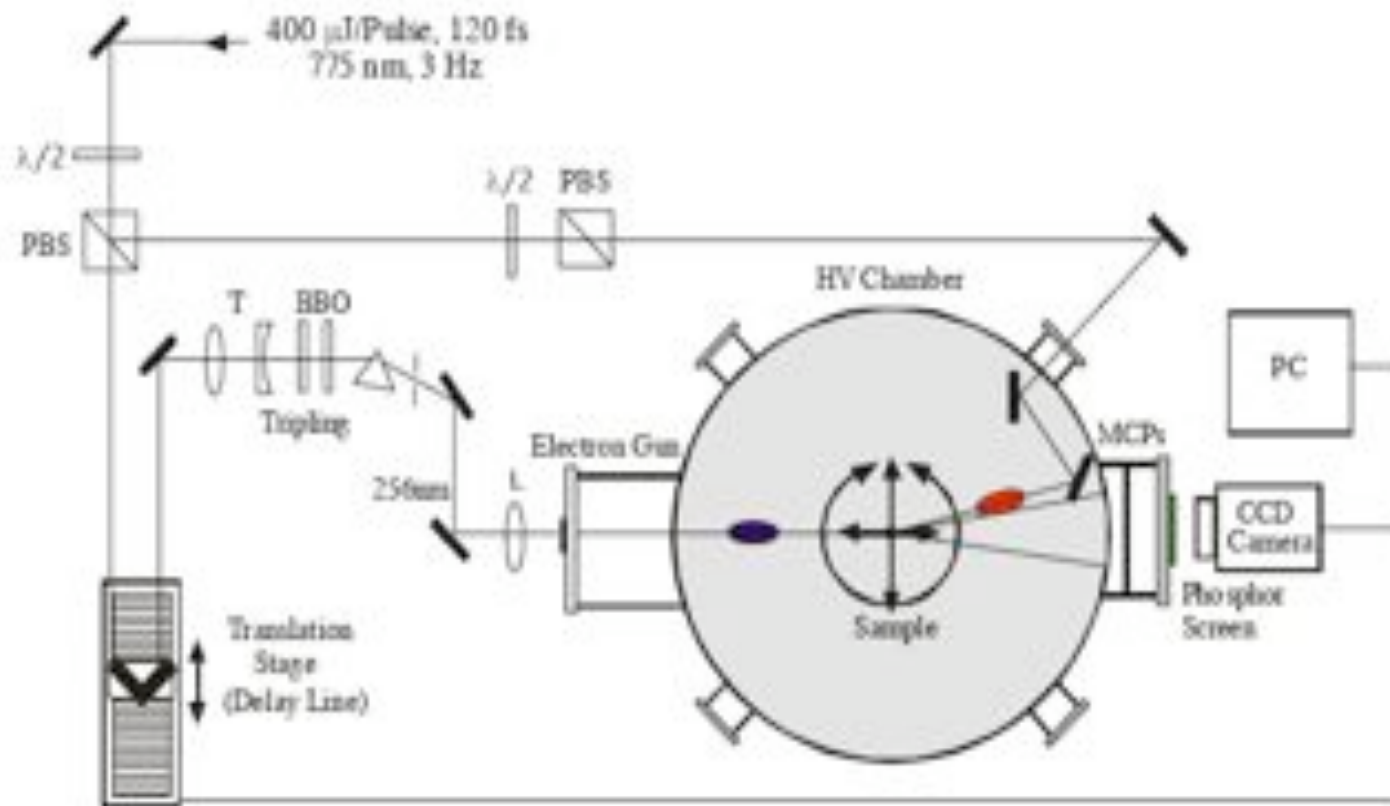
Photolyzed
Color-coded maps superimposed: MbCO at 100 ps

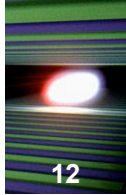






Ultrafast electron diffraction



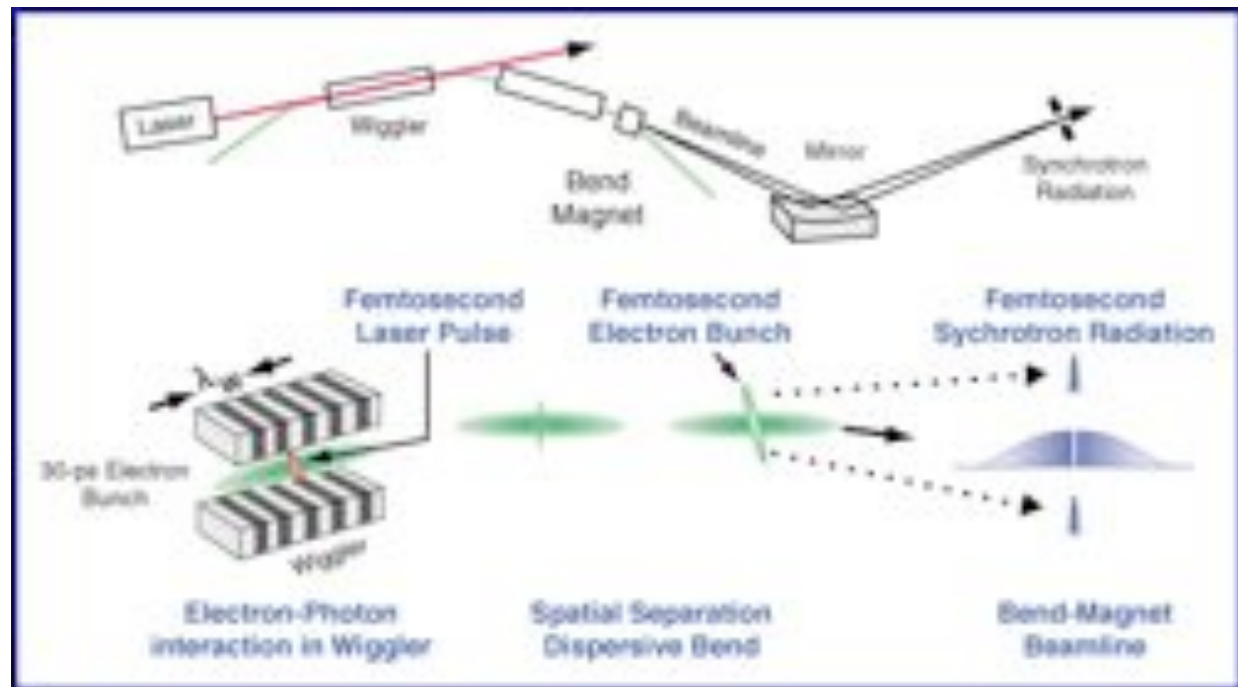


Laser-based: laser-plasma,
plasma-wiggler, HHG,...

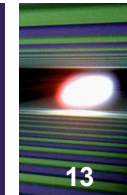
Accelerator-based:

Storage rings:

- bunch-slicing,
- bunch-rotation

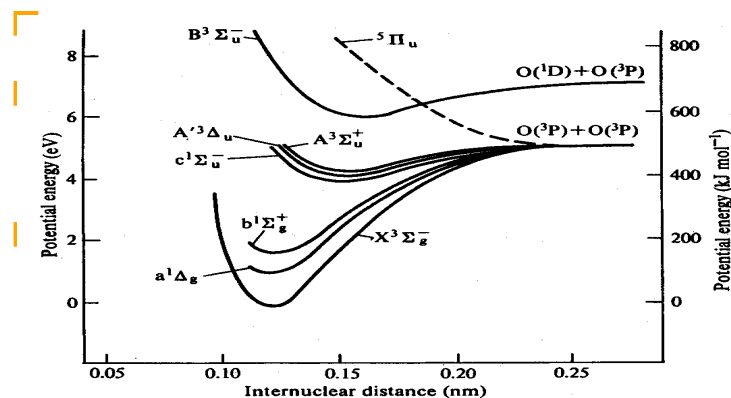


Wanted...A more brilliant X-ray source, with:



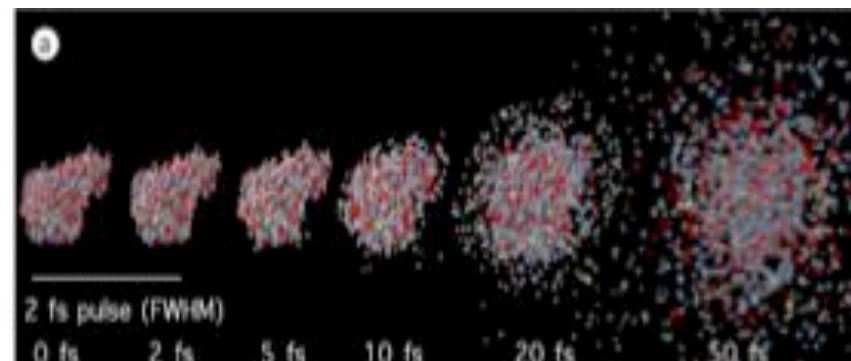
13

wavelength down to ~ 0.1 nm \Rightarrow atomic-scale resolution



ultrashort (<1 ps) pulses
 \Rightarrow "molecular movies"

ultra-high peak brightness
 \Rightarrow investigation of matter
under extreme conditions...



transverse spatial coherence

\Rightarrow imaging of single nanoscale objects, possibly down to individual macromolecules (no crystals)

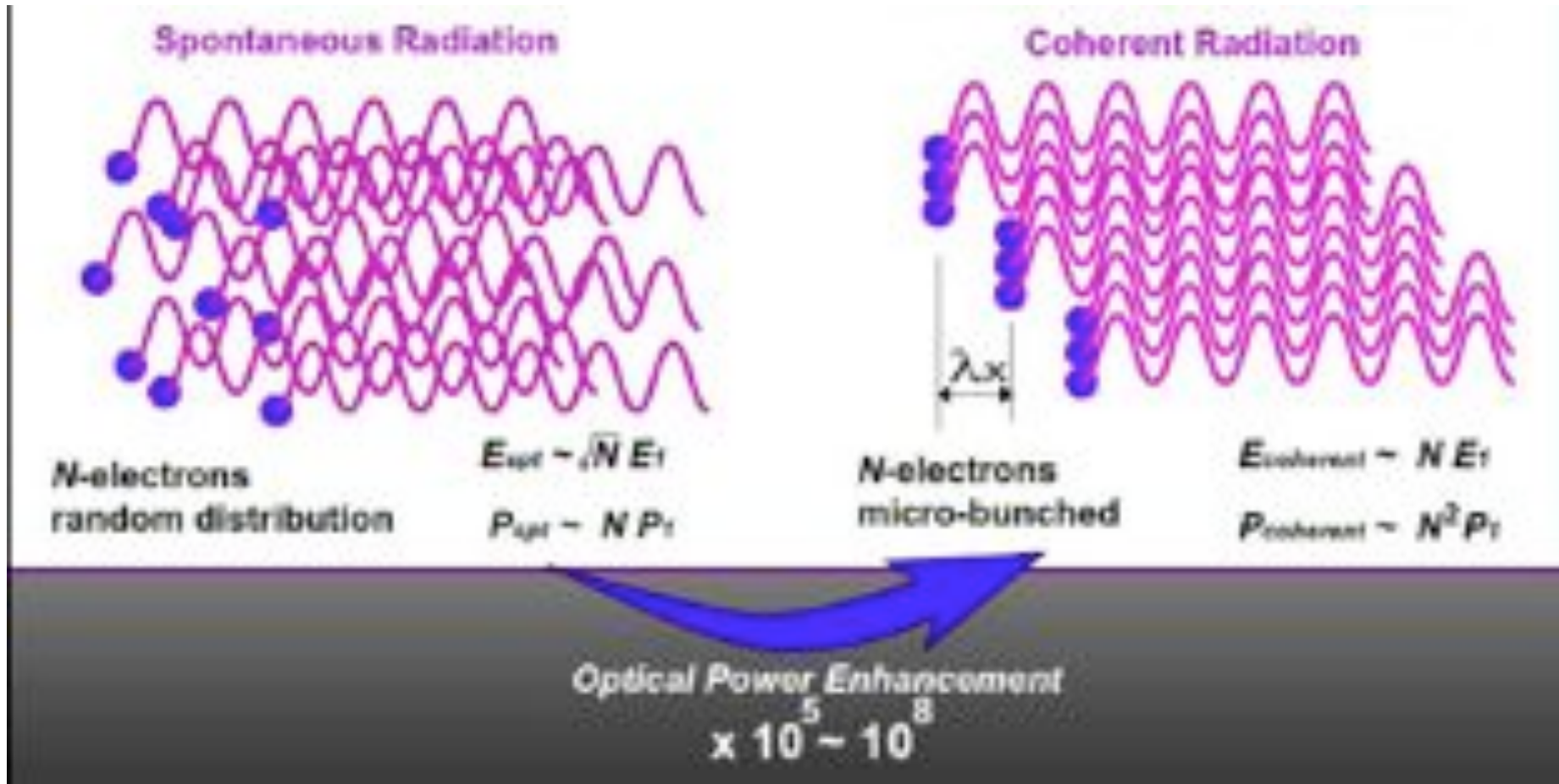
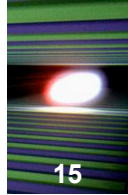


Compression of electron bunches to ~ 100 fs preserving (or even increasing) the brilliance and number of photons per bunch is impossible in a storage ring configuration, where the same electrons run through the undulators 10^5 to 10^6 times per second.

This can however be achieved in a single-pass machine such as a linear accelerator, with suitable bunch compressors.

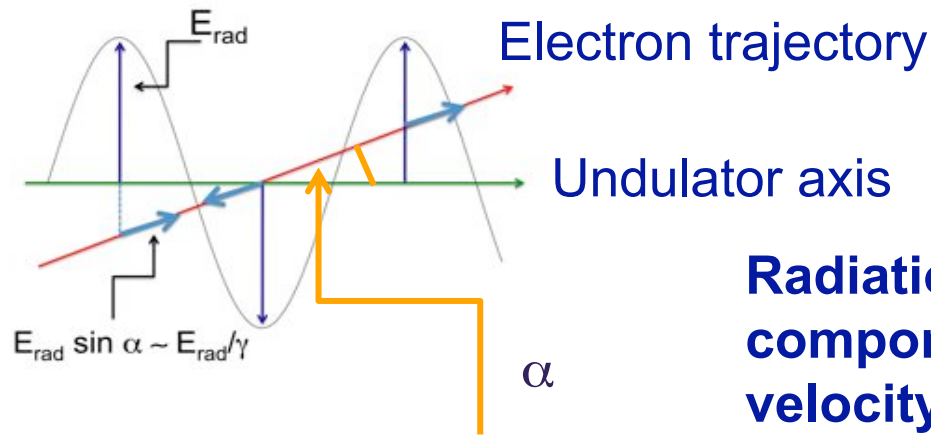
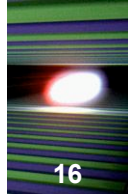
In addition, in a linac, emittance ε is NOT conserved, but $\varepsilon_n = \gamma\varepsilon \sim \text{const.}$, with $\gamma = E/mc^2$. It is then possible to reach the condition in which $\varepsilon \sim \lambda$.

Spontaneous vs. coherent rad. in Undulators

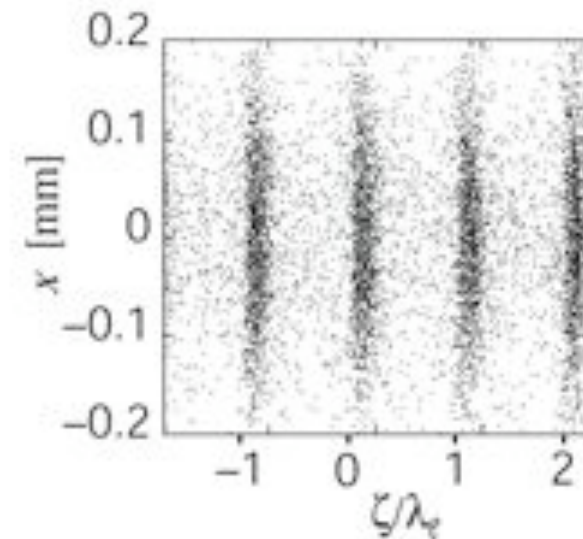
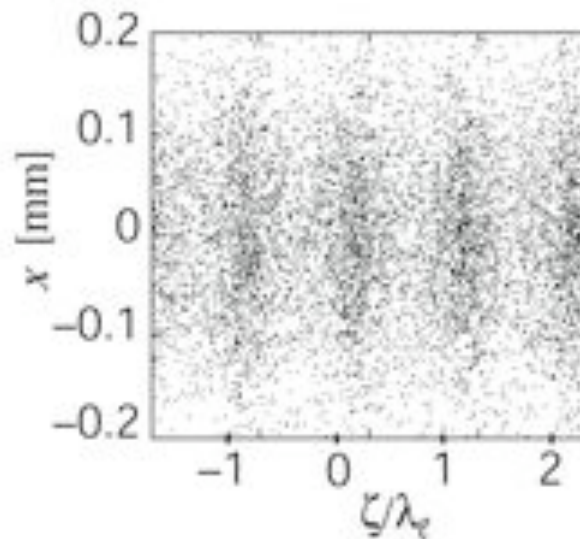
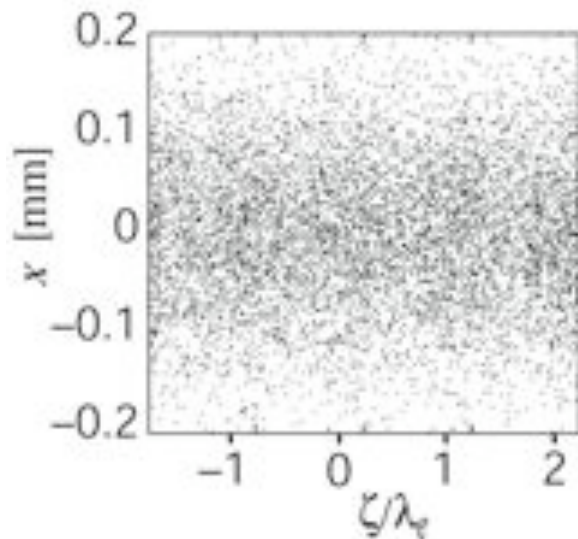


(after T. Shintake)

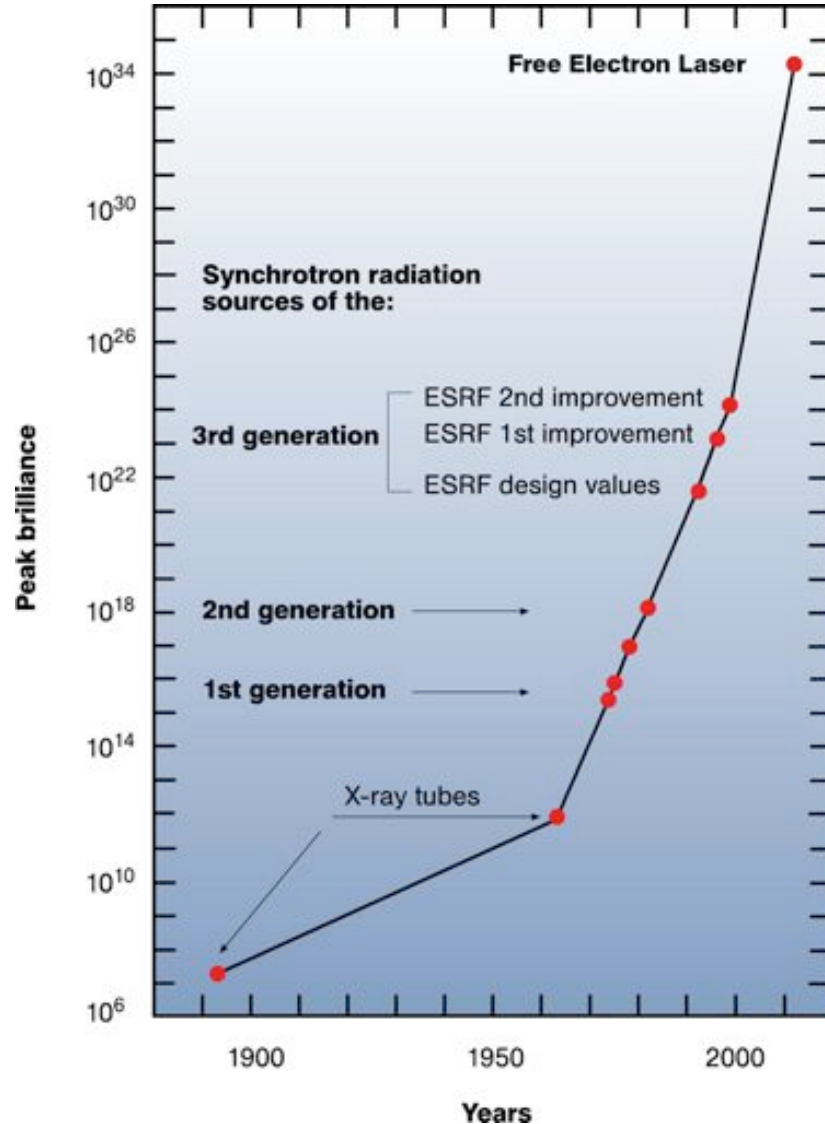
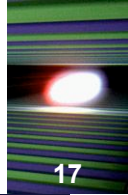
Origin of Microbunching



Radiation electric field has a small component parallel to electron velocity, which can accelerate or decelerate electrons

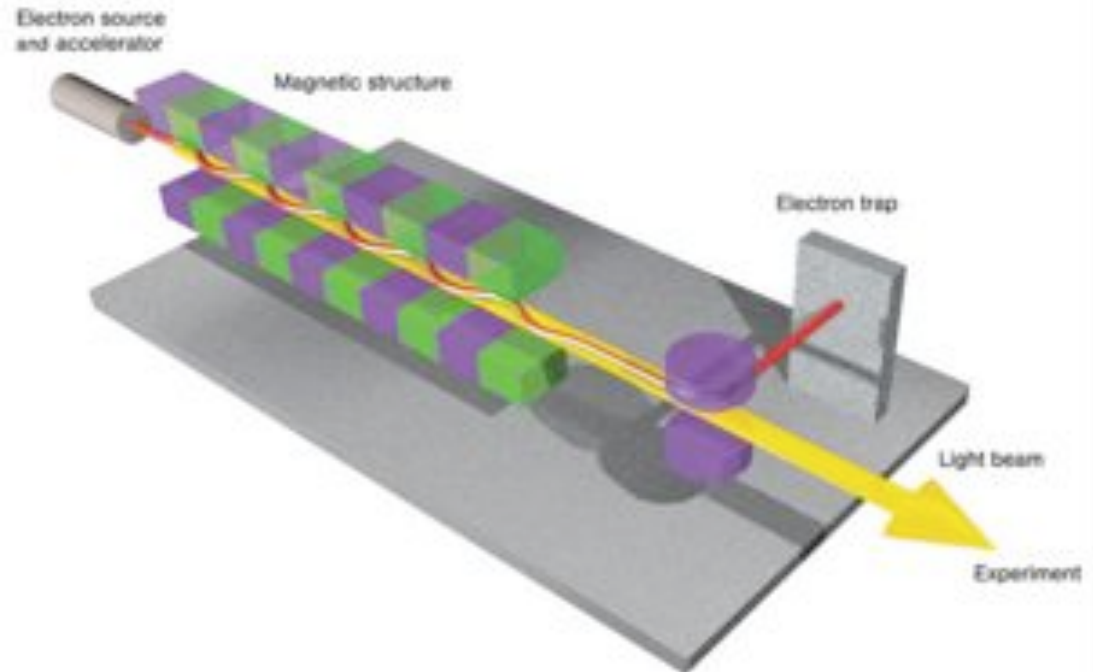


Peak brilliance of X-ray Sources vs. time



Free Electron Lasers:

- Based on Linear Accelerators
- Deliver ultrashort pulses
(100 fs = 0.1 ps = 10^{-13} s or less)
- (Transversely) Spatially coherent
(laser-like) radiation



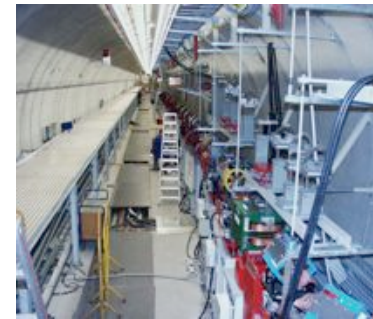
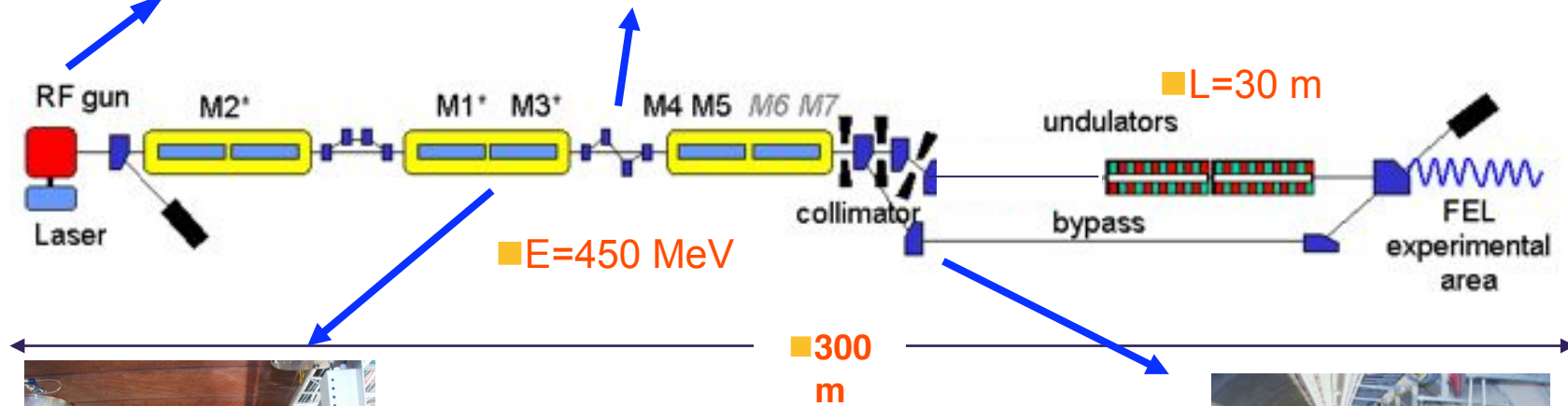
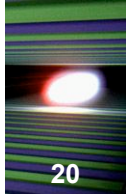


- **FLASH** – Ultraviolet and soft x-ray FEL user facility in Hamburg (down to $\lambda \sim 6.5$ nm) 10^{12} Ph/pulse
- **SCSS Test Accelerator** – Ultraviolet and soft x-ray FEL user facility at Spring 8, Japan ($\lambda \sim 30 - 60$ nm)
- First beam from **LCLS** (Linac Coherent Light Source), the X-ray FEL using 13.6 GeV electrons from SLAC Linac, Stanford, CA, on April 10, 2009 10^{12} Ph/pulse



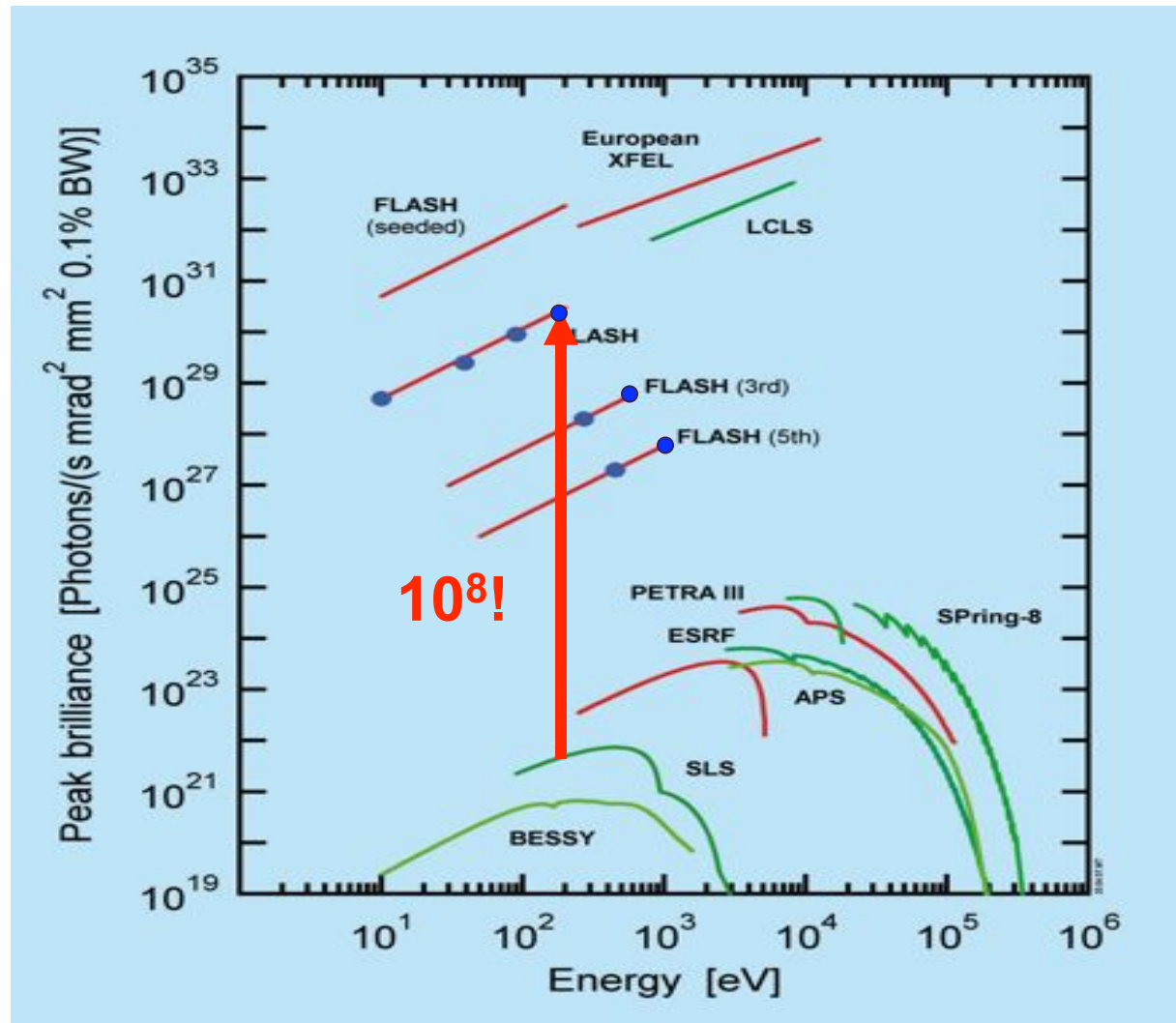
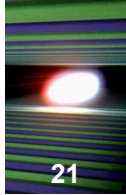
**The first SASE FEL
operating in the soft X-
rays, down to 6.5 nm
(+3rd, 5th harmonic!)**

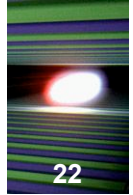
**1 GeV Superconducting
Linear Accelerator**



- Jan 2005: first lasing at 32 nm
- Aug 2005: first user exper.

Comparison of 3rd and 4th generation sources





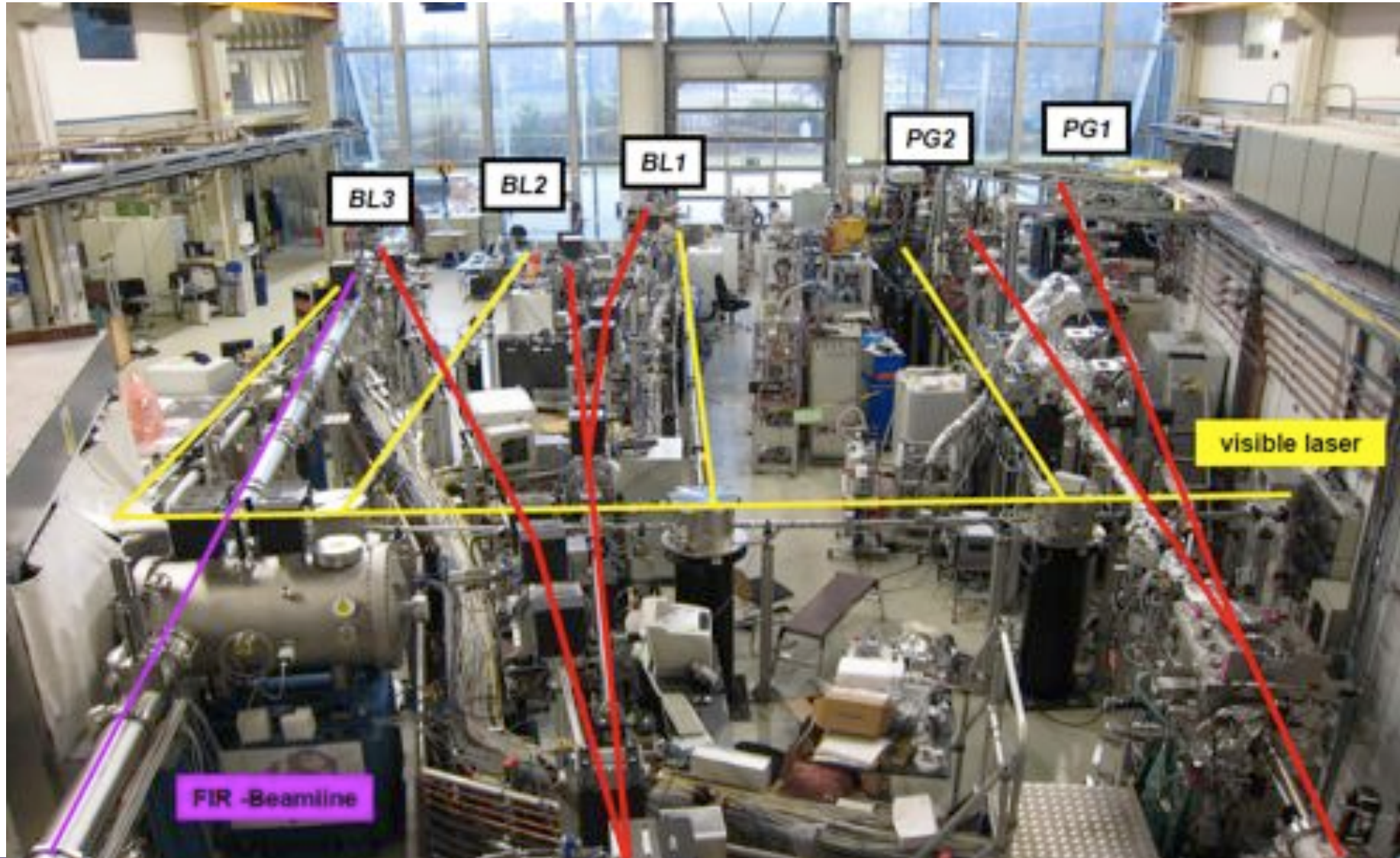
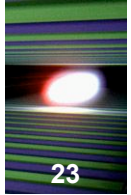
**The first SASE FEL
operating in the soft X-
rays, down to 6.5 nm**

(+3rd, 5th harmonic!)

**1 GeV Superconducting
Linear Accelerator**



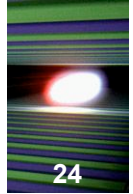
FLASH Experimental Hall



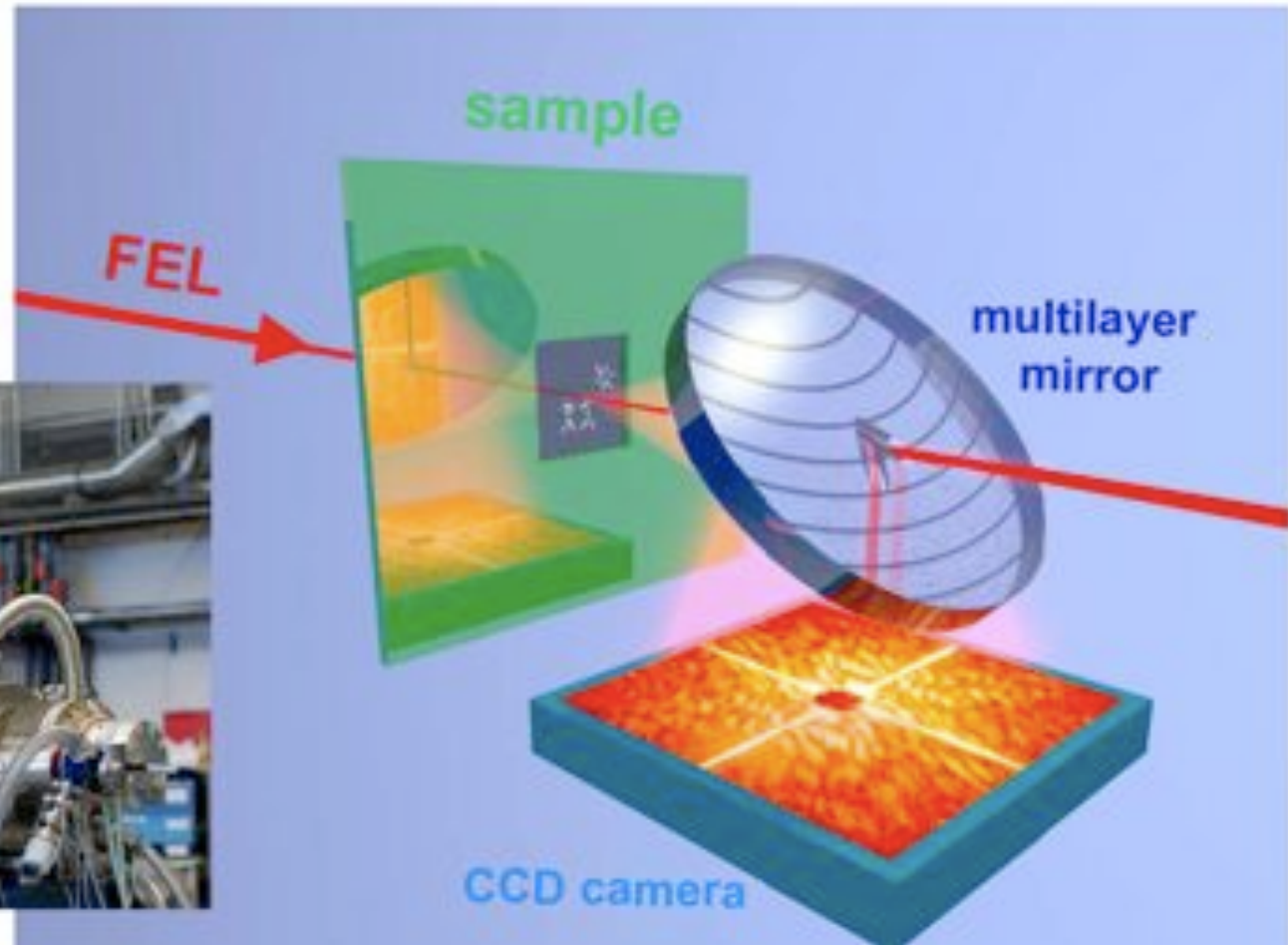
Trieste, 06.05.2010

Massimo Altarelli, European XFEL GmbH, Hamburg

Single-shot (~ 25 fs, $\lambda \sim 32$ nm) imaging

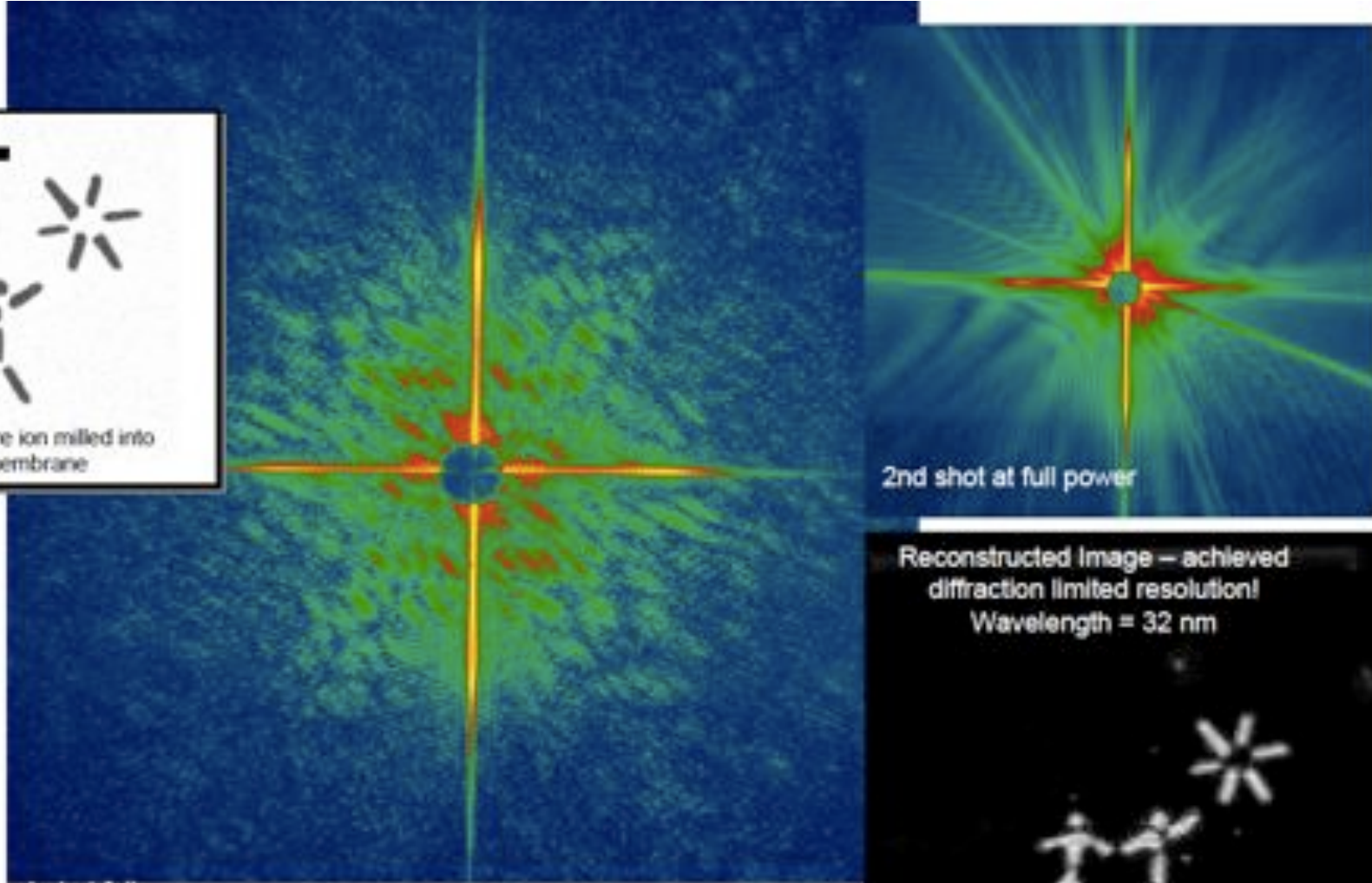
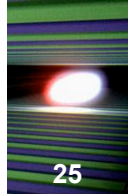


24



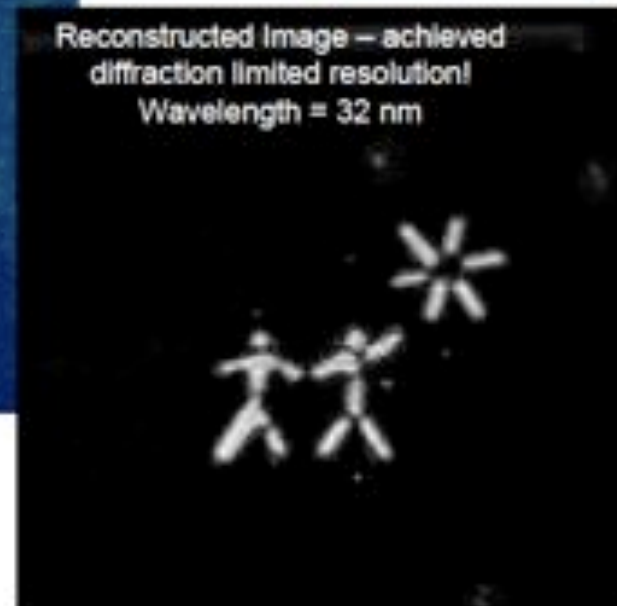
H. Chapman, J. Hajdu et al., *Nature Physics* **2**,
839 - 843 (2006)

Reconstructed Image - 62 nm resolution



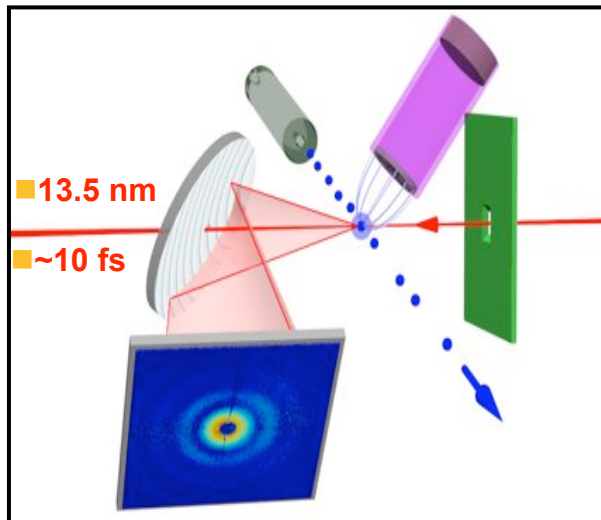
2nd shot at full power

Reconstructed Image — achieved
diffraction limited resolution!
Wavelength = 32 nm

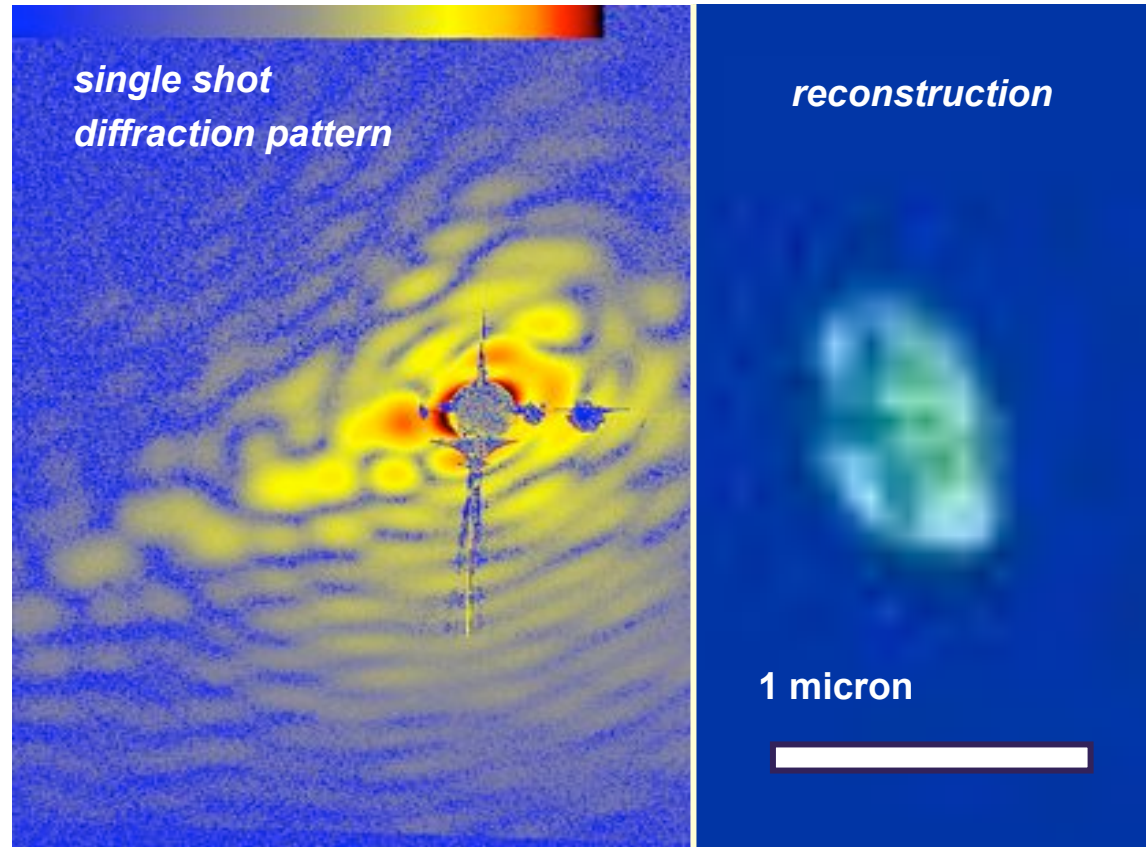


Imaging picoplankton organism "on the fly"

■ **PICOPLANKTON** are the most abundant **photosynthetic cells** in the oceans (discovered in 1988)



■ This cell was injected into vacuum from solution, and shot through the beam at 200 m/s

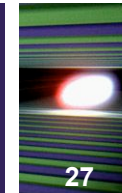


- J. Hajdu, I. Andersson, M. Svenda, M. Seibert (Uppsala)
- S. Boutet (SLAC)
- M. Bogan, H. Benner, U. Rohner, H. Chapman (LLNL)



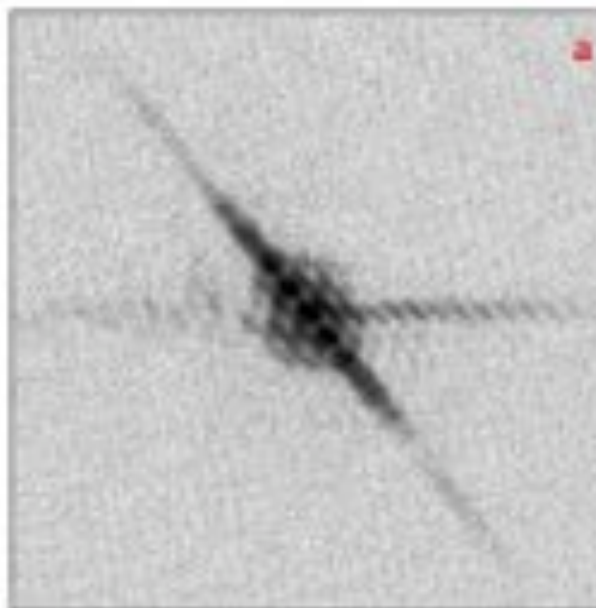
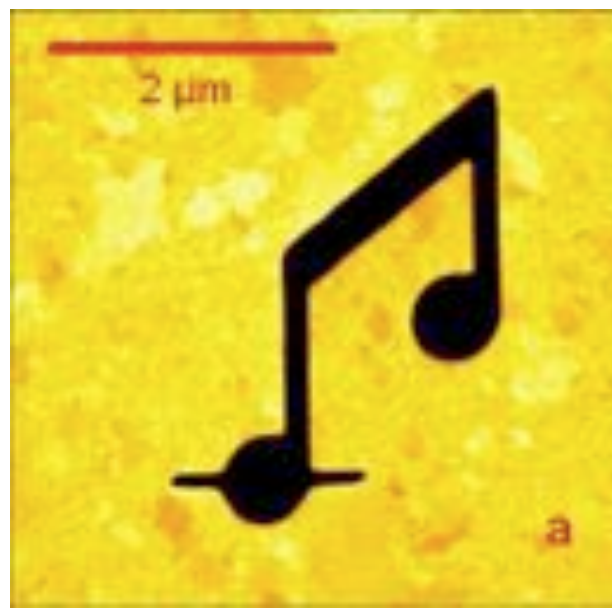
Stanford
Linear
Accelerator
Center

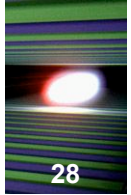




Single-Shot Diffractive Imaging with a Table-Top Femtosecond Soft X-Ray Laser-Harmonics Source

A. Ravasio,¹ D. Gauthier,¹ F. R. N. C. Maia,² M. Billon,¹ J-P. Caumes,¹ D. Garzella,¹ M. Géléoc,¹ O. Gobert,¹ J-F. Hergott,¹ A-M. Pena,¹ H. Perez,¹ B. Carré,¹ E. Bourhis,³ J. Gierak,³ A. Madouri,³ D. Mailly,³ B. Schiedt,³ M. Fajardo,⁴ J. Gautier,⁵ P. Zeitoun,⁵ P. H. Bucksbaum,⁶ J. Hajdu,^{2,6} and H. Merdji^{1,6,*}





LETTERS

Injection of harmonics generated in gas in a free-electron laser providing intense and coherent extreme-ultraviolet light

G. LAMBERT^{1,2,3*}, T. HARA^{2,4}, D. GARZELLA¹, T. TANIKAWA², M. LABAT^{1,3}, B. CARRE¹, H. KITAMURA^{2,4}, T. SHINTAKE^{2,4}, M. BOUGEARD¹, S. INOUE⁴, Y. TANAKA^{2,4}, P. SALIERES¹, H. MERDJI¹, O. CHUBAR³, O. GOBERT¹, K. TAHARA² AND M.-E. COUPRIE³

¹Service des Photons, Atomes et Molécules, DSM/DRECAM, CEA-Saclay, 91191 Gif-sur-Yvette, France

²RIKEN SPring-8 Centre, Harima Institute, 1-1-1, Koto, Sayo-cho, Sayo-gun, Hyogo 679-5148, Japan

³Groupe Magnétisme et Insertion, Synchrotron Soleil, L'Orme des Merisiers, Saint Aubin, 91192 Gif-sur-Yvette, France

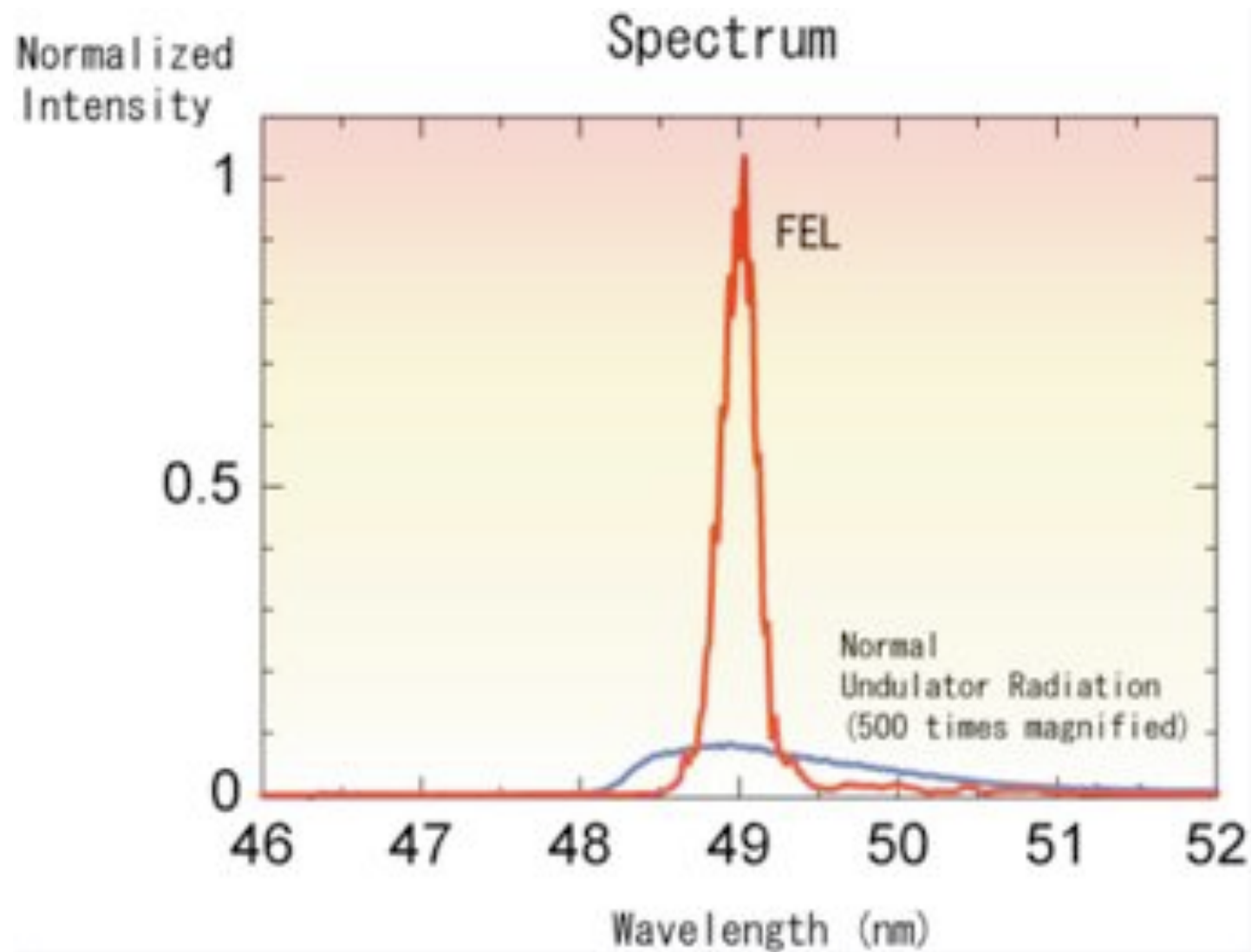
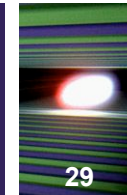
⁴XFEL Project Head Office/RIKEN, 1-1-1, Koto, Sayo-cho, Sayo-gun, Hyogo 679-5148, Japan

*e-mail: guillaume.lambert@synchrotron-soleil.fr

Nature Physics 4, 296 - 300 (01 Apr 2008)

Published online: 9 March 2008; doi:10.1038/nphys889

SASE at the SCSS test facility



150 MeV
Linac

Experimental Layout for HHG

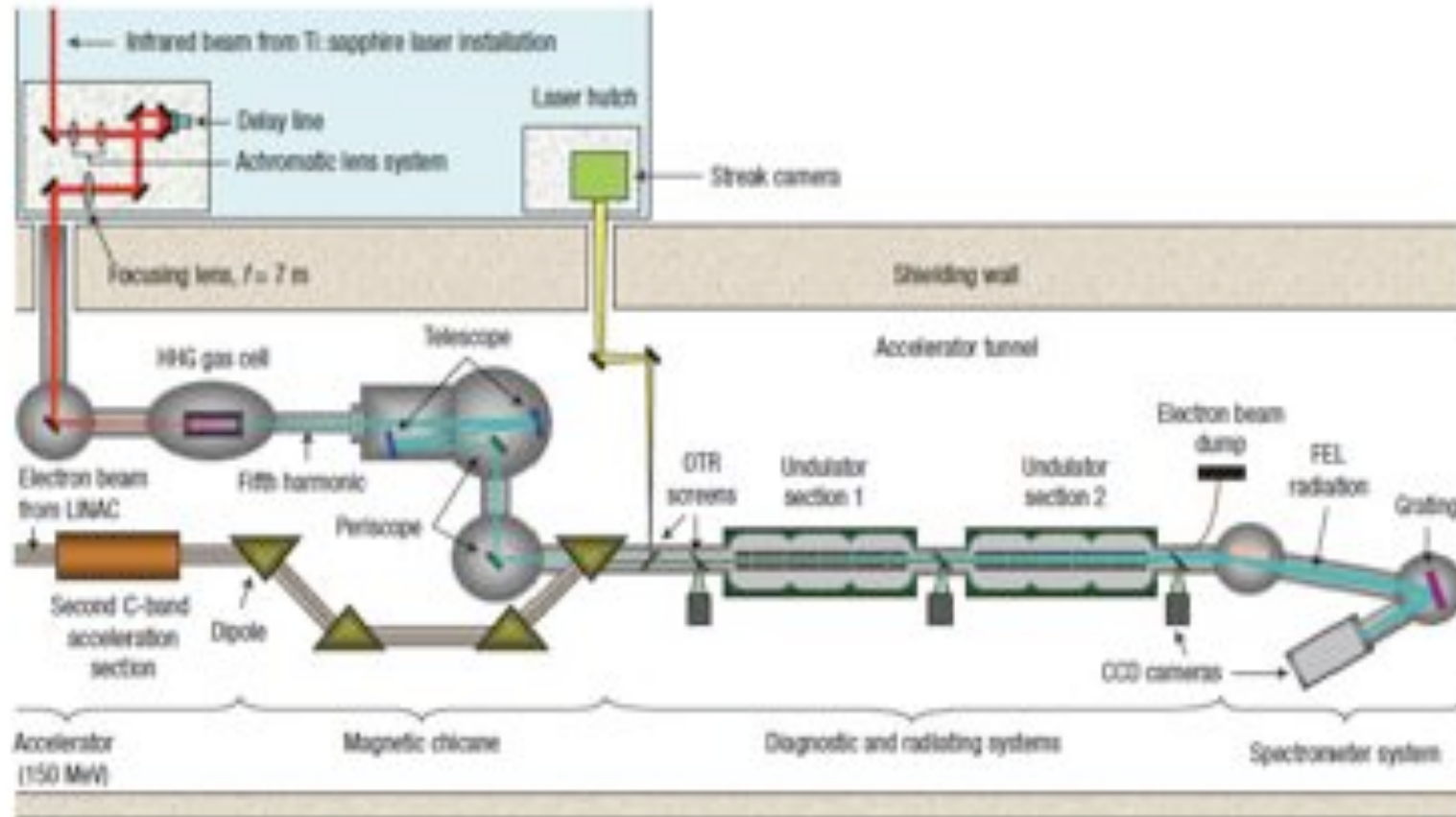
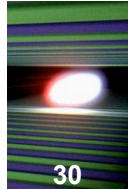


Figure 1 Layout of the experiment. A Ti:sapphire laser (800 nm, 20 mJ, 100 fs FWHM, 10 Hz) is loosely focused into a xenon gas cell (focal length $f = 7$ m), optimizing HHG output. Using the telescope and periscope optics (CaF₂ mirrors), the HHG seed beam is spectrally selected, refocused and spatially and temporally overlapped with the electron beam (150 MeV, 1 ps FWHM, 10 Hz—LINAC stands for linear accelerator) in the two consecutive undulator sections 1 and 2, which are both tuned to 160 nm, corresponding to the fifth harmonic of the laser. The beam position is monitored on optical transition radiation (OTR) screens.

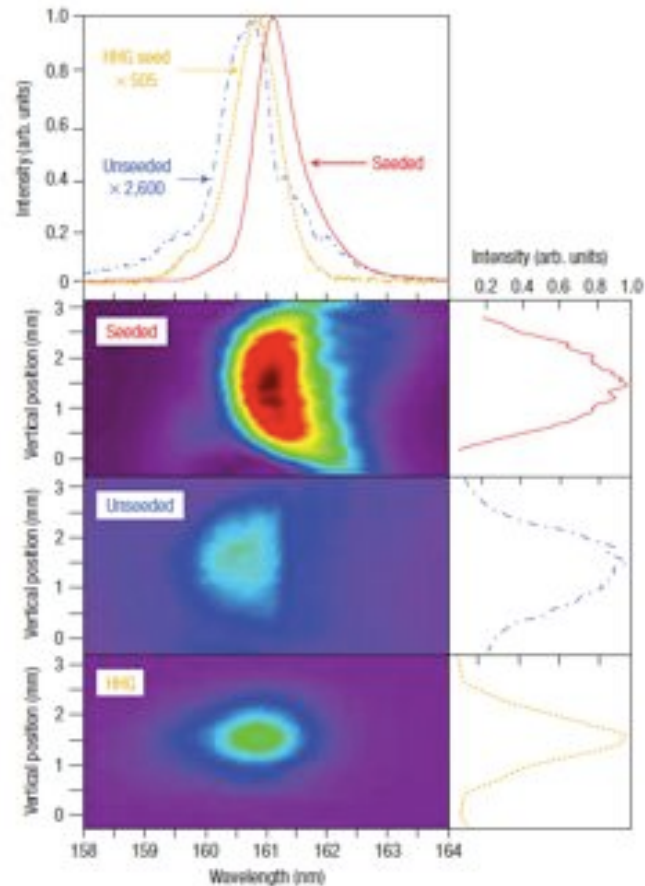


Figure 2 Comparison between the FEL seeded emission, the unseeded emission and the HHG seed at the fundamental wavelength (160 nm). The spatial (vertical) and spectral distributions are mapped on the CCD (charge-coupled device) camera of a spectrometer; spatial (right) and spectral (up) profiles are plotted at maximum intensity. The lines correspond to the seeded (single shot, line) and unseeded emission (averaged on 10 shots, dash-dot) and the HHG seed (single shot, dots). The seed pulse energy was 0.53 nJ and only the first undulator section was used for amplifying the HHG pulse.

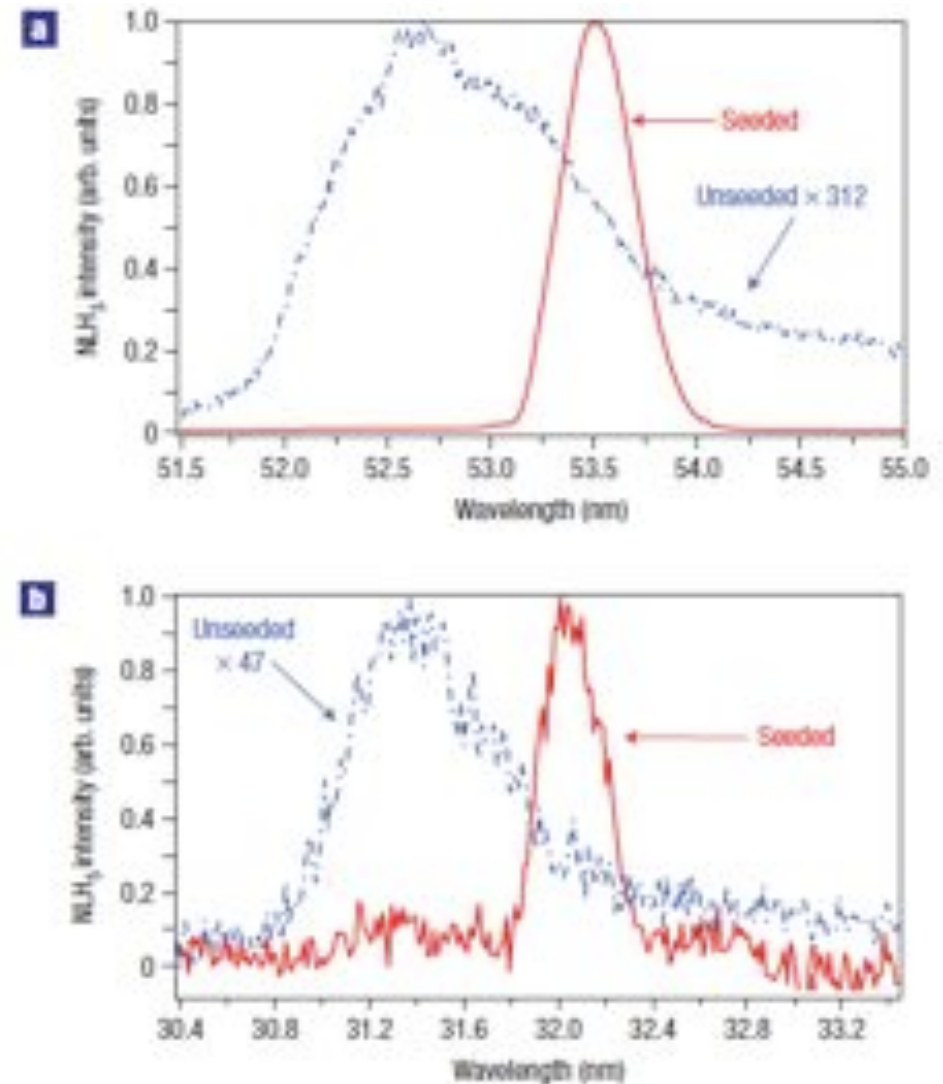
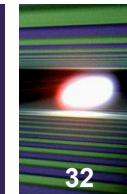


Figure 3 Spectra of the FEL seeded and unseeded emission at the wavelengths of the third and fifth NLHs. The spectra have been obtained by integrating the two-dimensional distributions of the CCD images (as for Fig. 2) over the vertical dimension. The seeded (single shot, line) and unseeded (averaged on 10 shots, dash-dot) FEL emissions are plotted for the third (a) and fifth (b) NLHs. The seed pulse energy was 0.53 nJ and only the first undulator section was used for radiating the NLHs.



1.5 Å
Coherent
X-rays!!

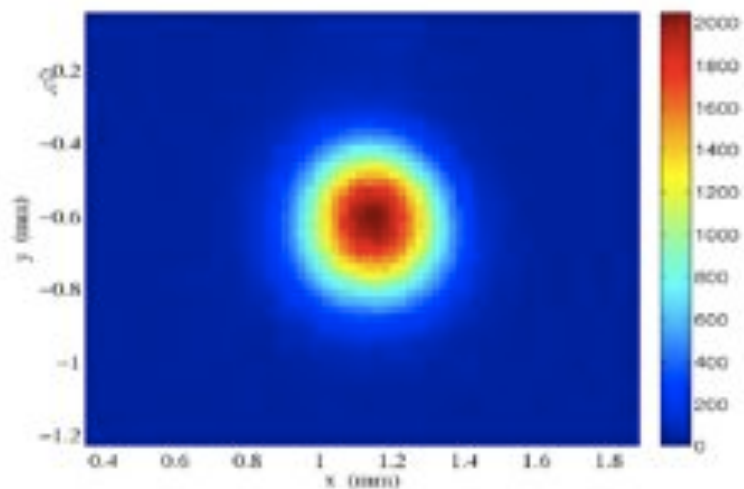
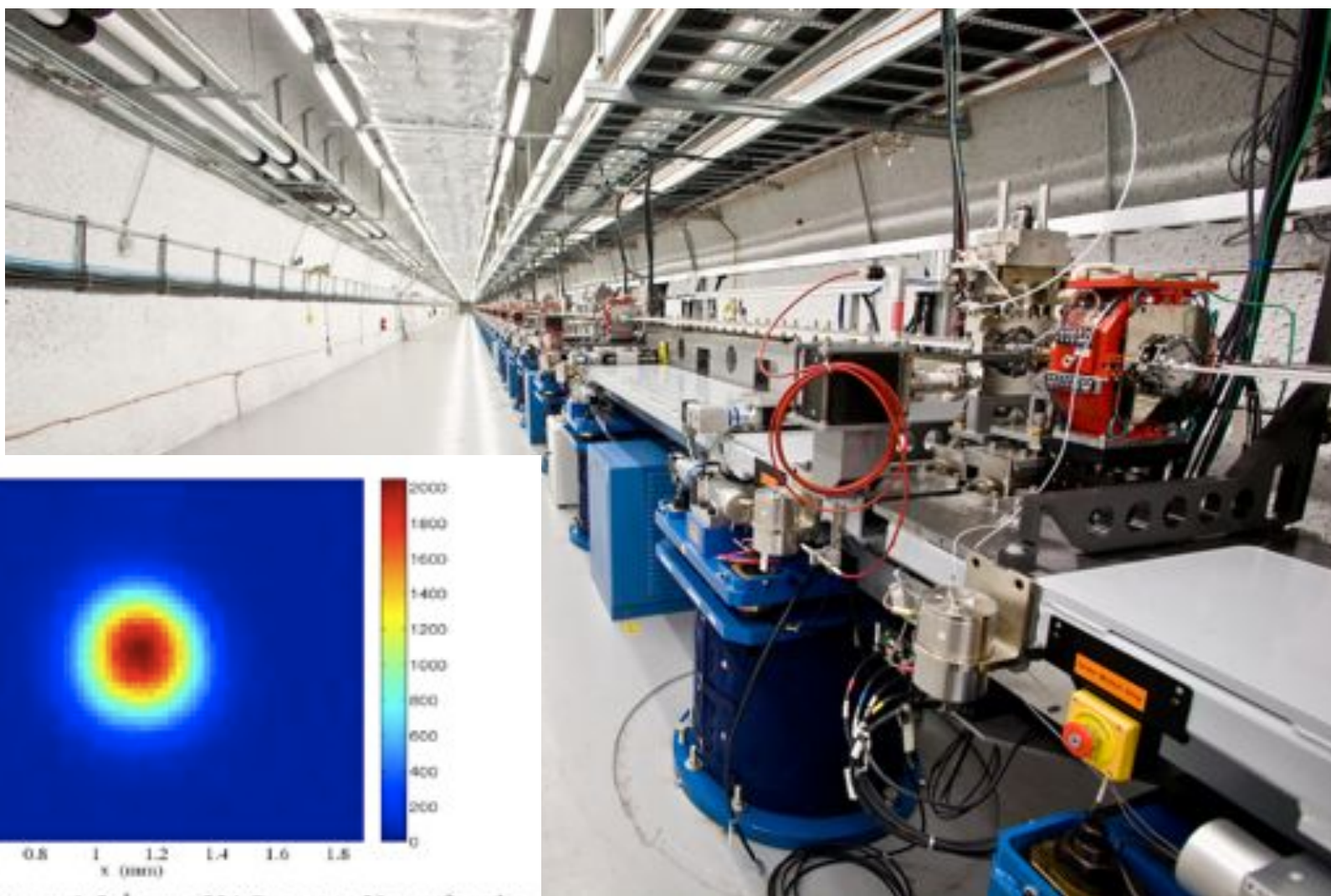
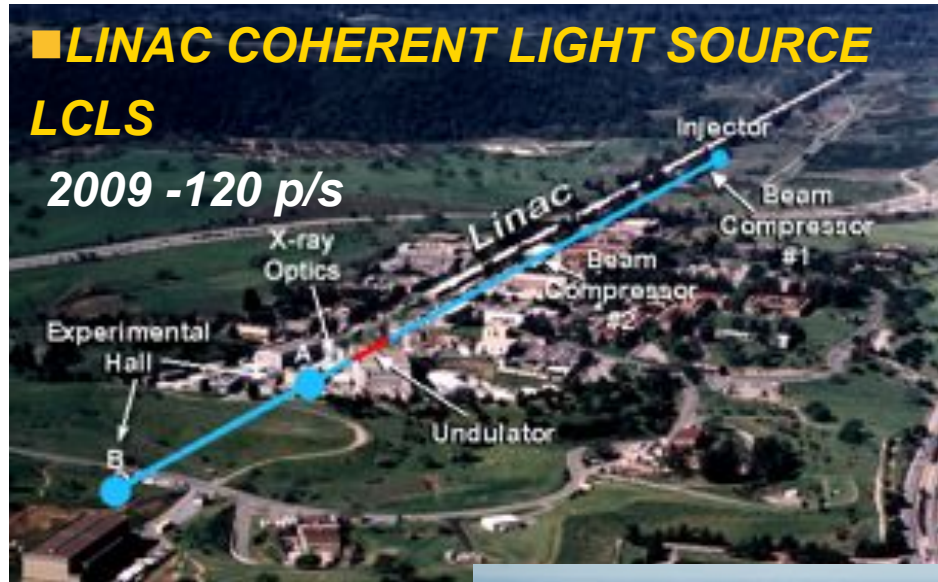
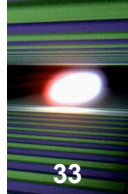
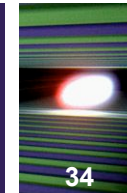


Figure 10: FEL x-rays at 1.5 Å on a YAG screen 50 m after the last inserted undulator (see Table 1 for measured parameters).

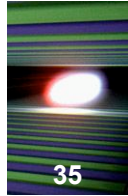
Hard x-ray FEL Projects



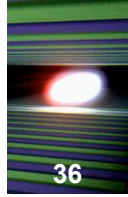


Trieste, 06.05.2010

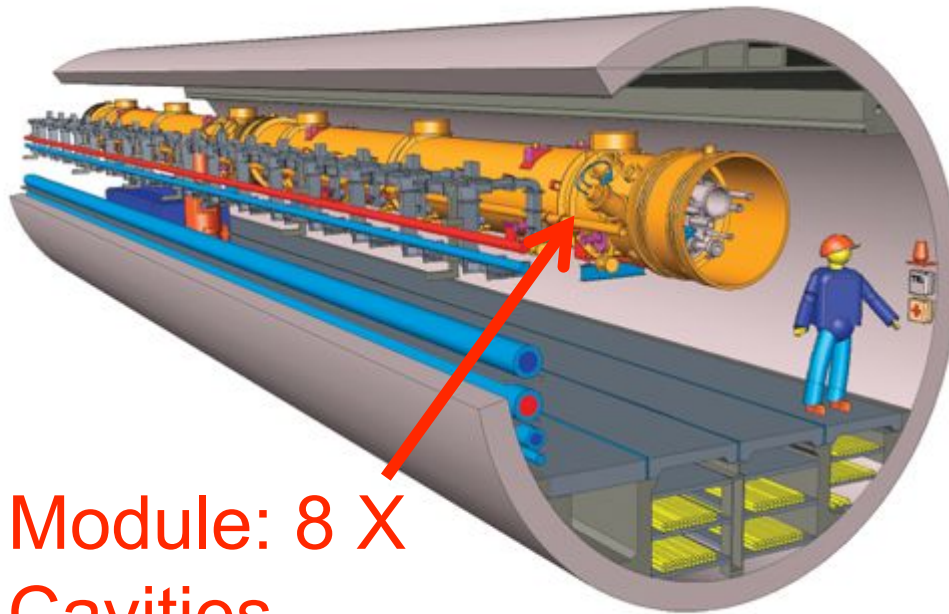
Massimo Altarelli, European XFEL GmbH, Hamburg



Superconducting "TESLA" Technology

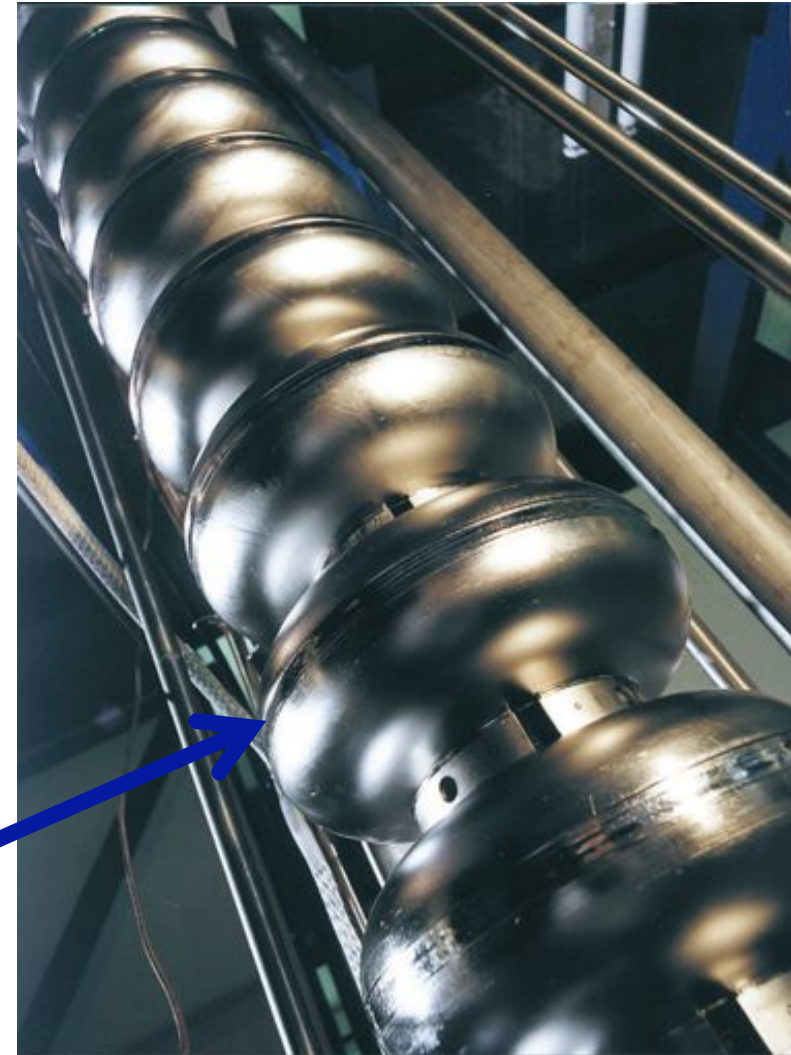


**100 8-Cavity modules, 1.4 km,
17.5 GeV Electron Energy**



**Module: 8 X
Cavities**

Niobium Cavities

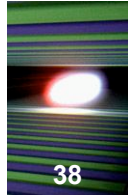


Module PXFEL1 on the test bench

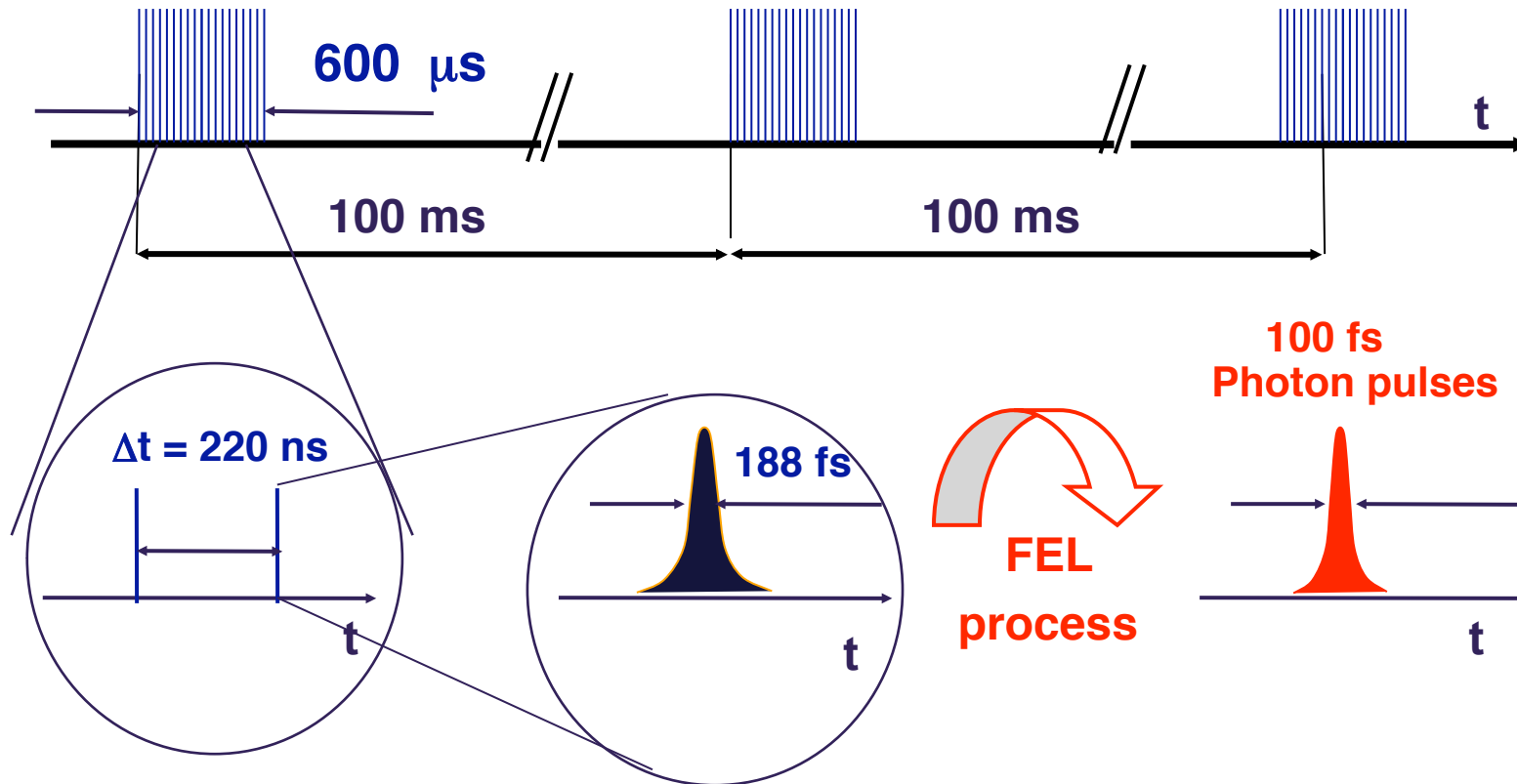


China
France
Germany
Italy
Spain

Photo:
D. Kostin,
DESY

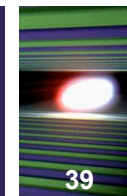


Electron bunch trains (with up to 2700 bunches à 1 nC)

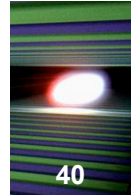


Alternatively: 20 bunch trains / second, 300 μs long, with up to 1350 bunches each...

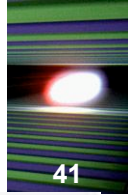
Comparison of the X-ray FEL Projects



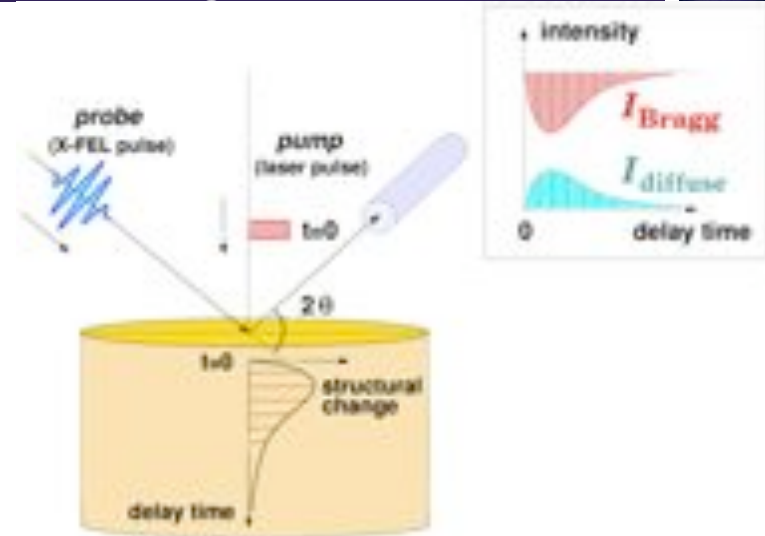
	<i>LCLS (USA)</i>	<i>SCSS (JAPAN)</i>	<i>EUROPEAN XFEL (SASE1)</i>
<i>Max. Electron Energy (GeV)</i>	14.3	8.0	17.5
<i>Minimum Wavelength(nm)</i>	0.15	0.13	0.10
<i>Peak Brilliance</i>	1.5 10 ³³	1. 10 ³³	5. 10 ³³
<i>Average Brilliance</i>	4.5 10 ²²	1.5 10 ²³	1.6 10 ²⁵
<i>Pulses/s</i>	120	60	27 000
<i>Photons/pulse</i>	10 ¹²	2 10 ¹¹	10 ¹²
<i>First Beam</i>	2009	2011	2014



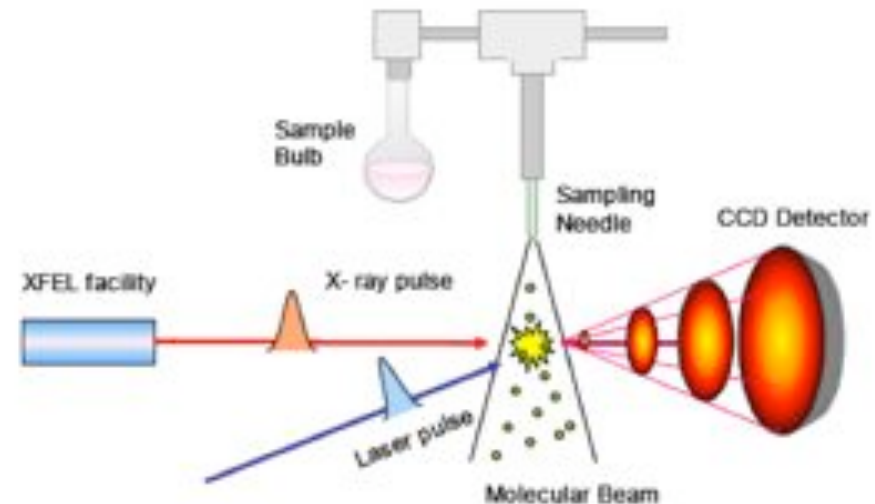
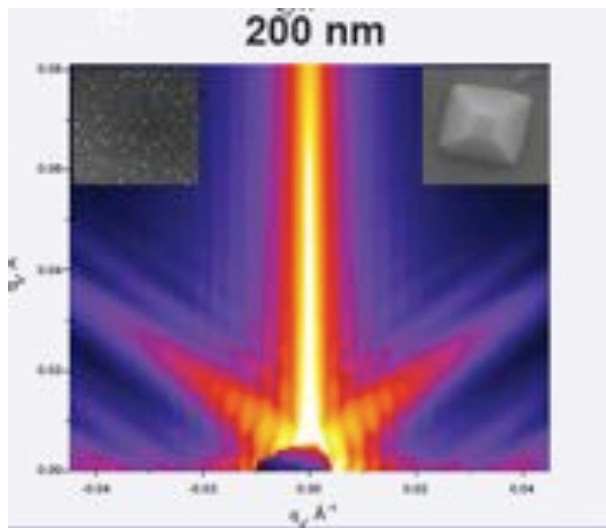
- Time-resolved, pump-and-probe experiments
- Coherent-diffraction imaging of nanoscale objects, down to *single macromolecules*
- Speckle Scattering and Photon-Correlation Spectroscopy
- High Energy-Density science



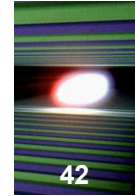
- Time-resolved, pump-and-probe experiments



- Coherent-diffraction imaging of nanoscale objects, down to *single macromolecules*

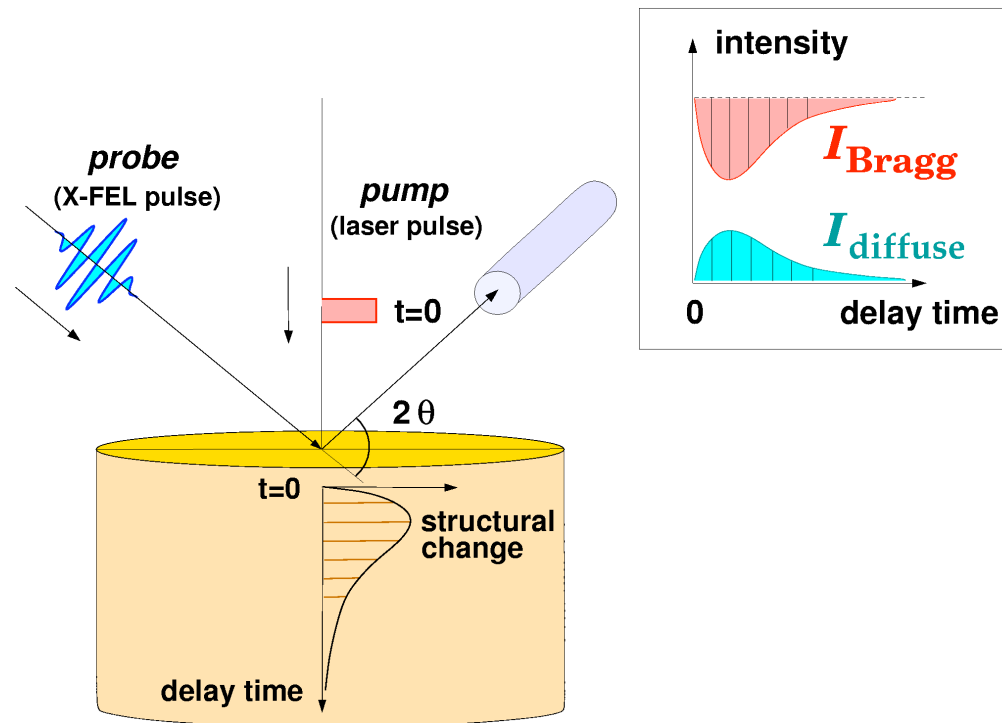


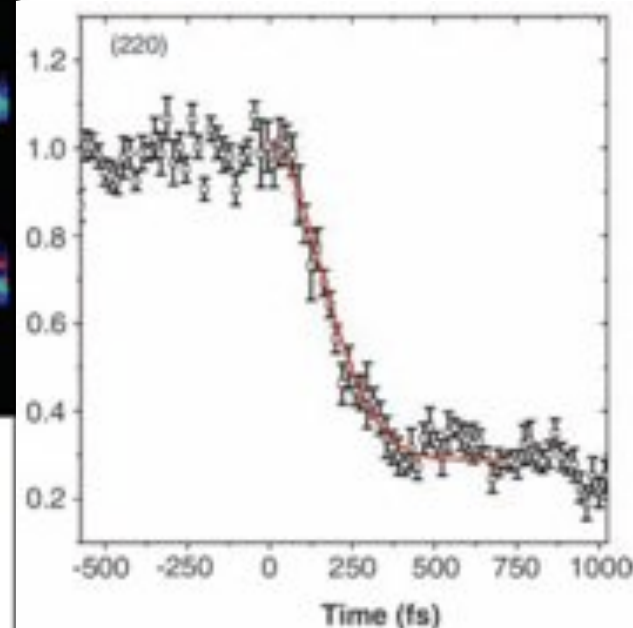
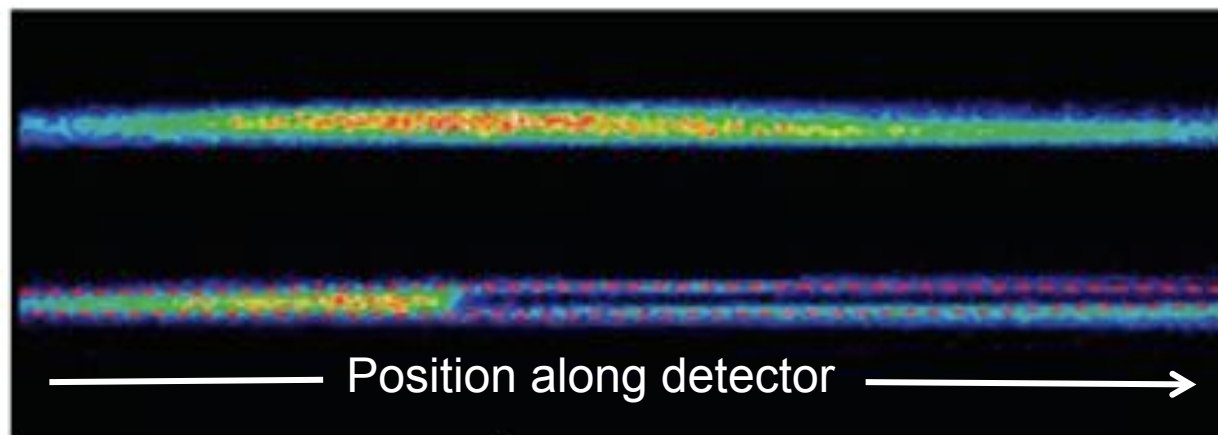
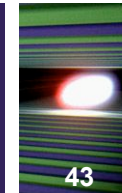
Pump and Probe Experiments



Today: study (structure) and dynamics on a
ns to ps timescale

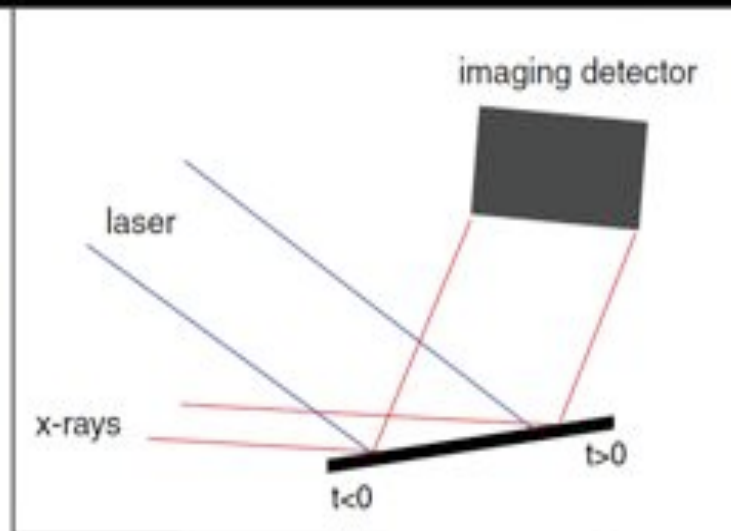
XFEL: study (structure) and dynamics on a
ps to fs scale





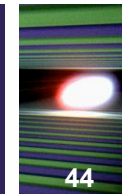
(220) Reflection
intensity as a function
of time

Fig. 1. (Top) A single-shot image of scattered x-rays from unperturbed sample above a single-shot image of perturbed sample. Dashed curves show region excited by laser pulse. (Bottom) Experimental setup showing cross-beam topography technique. By crossing the pump and probe beams on the sample and imaging the diffracted x-rays, we mapped temporal information into spatial information, enabling collection of the complete time history around time zero in a single shot. Time runs from left to right. The time window shown is ~ 8 ps.



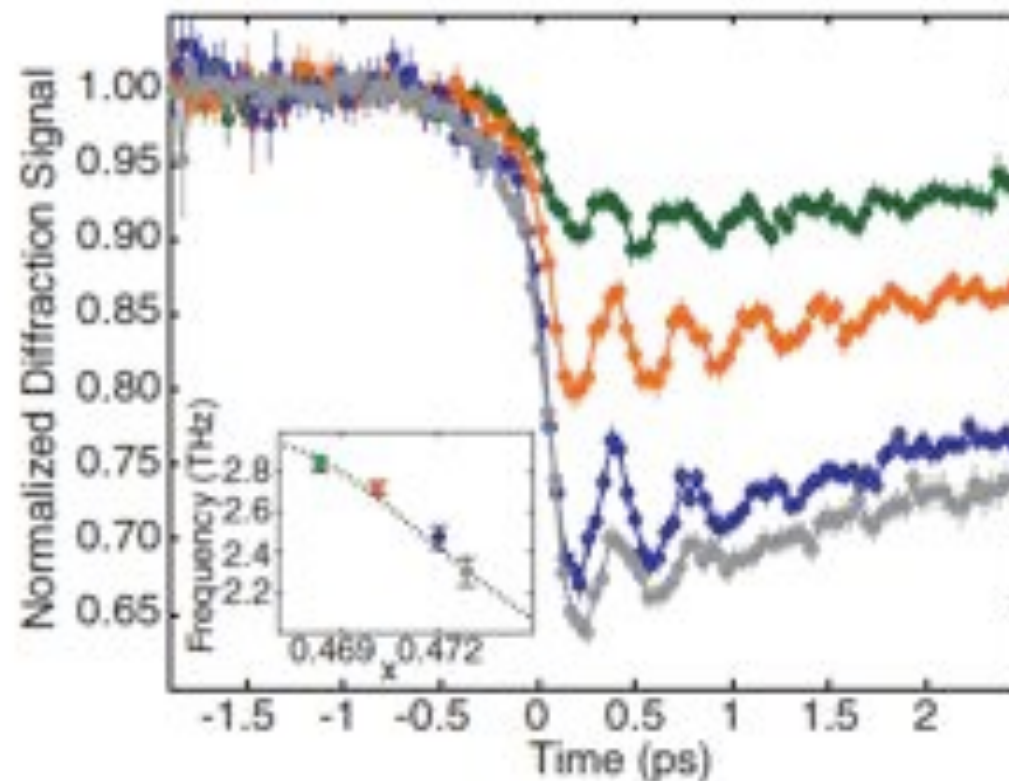
A.M. Lindenberg *et al.*, Science **308**, 392 (2005)

Ultrafast bond-softening in Bi (SPPS)

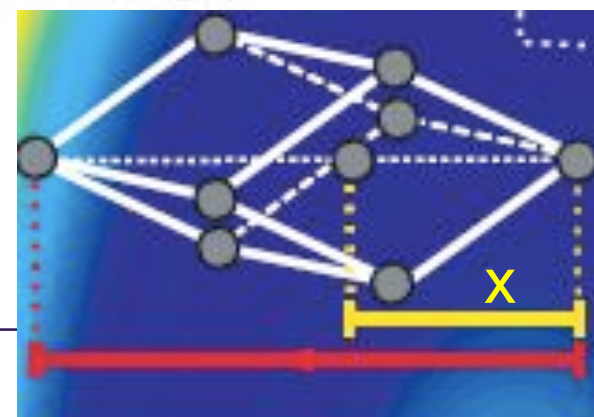


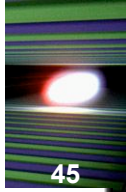
44

Fig. 1. Bismuth (111) x-ray diffraction efficiency as a function of time delay between the optical excitation pulse and x-ray probe for excitation fluences of 0.7 (green), 1.2 (red), 1.7 (blue), and 2.3 mJ/cm² (gray). The zero-delay point was set at the half maximum of the initial transient drop. The inset displays the optical phonon frequency as a function of the normalized atomic equilibrium position along the body diagonal of the unit cell x as measured by x-ray diffraction. The dotted curve represents the theoretical prediction obtained from DFT calculations of the excited-state potential-energy surface (10).



D.M. Fritz et al., Science, 315, 633 (2007)



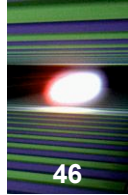


Nature **459**, 24 (7 May 2009)

STRUCTURES OF DESIRE

What do protein crystallographers dream of? The eukaryotic ribosome, the spliceosome, the nuclear-pore complex, the HIV trimer and almost any transmembrane protein, finds **Ananyo Bhattacharya**.

....Wayne Hendrickson of Columbia University in New York says there is also a lot of excitement about technologies that might be possible at facilities such as the European XFEL (X-Ray Free Electron Laser) under construction in Hamburg, Germany ...The idea here is that an extremely short burst of X-rays could be scattered off a single protein molecule, blowing it apart but revealing something about its structure before the disintegration. "You are in principle able to capture the molecule in action," Hendrickson says....

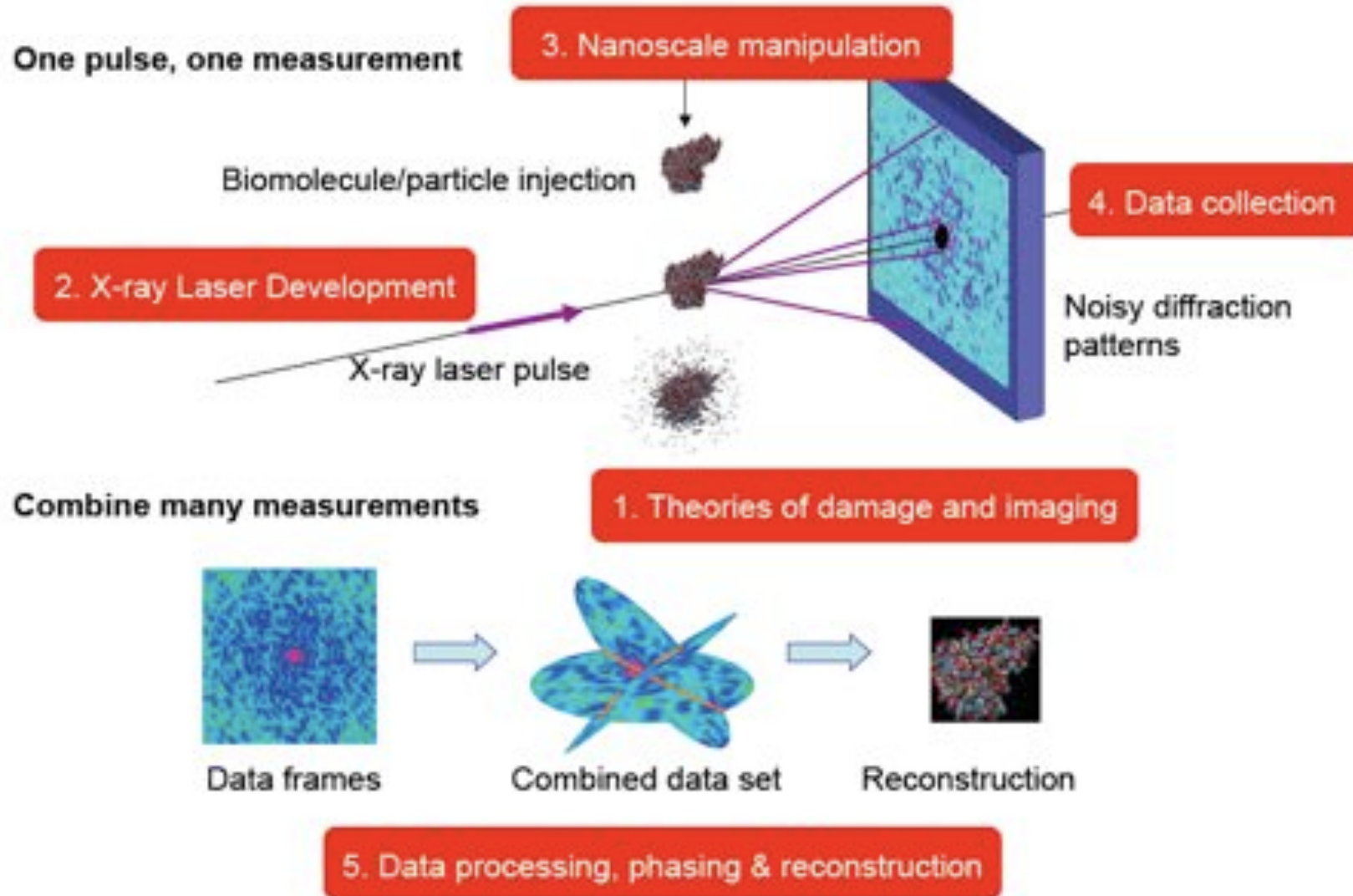
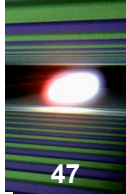


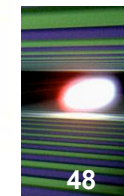
Problems with conventional imaging in biology:

- (1) Inability to obtain high resolution structures for non-reproducible objects of any type
- (2) Problems with large reproducible objects
- (3) Problems with crystallography
 - Resolution depends on crystal quality (1D, 2D and 3D cryst.)
 - Does it crystallise at all?
- (4) Problems with the 4th dimension

Ultra-fast coherent scattering carries promise here

Single-Molecule X-ray Imaging





Structure from fleeting illumination of faint spinning objects in flight

Russell Fung, Valentin Shneerson, Dilano K. Saldin and Abbas Ourmazd*

Moves are afoot to illuminate particles in flight with powerful X-ray bursts, to determine the structure of single molecules, viruses and nanoparticles. ... Using a new approach, we demonstrate the recovery of the structure of a weakly scattering macromolecule at the anticipated next-generation X-ray source intensities. Our work closes a critical gap in determining the structure of single molecules and nanoparticles by X-ray methods, and opens the way to reconstructing the structure of spinning, or randomly oriented objects at extremely low signal levels.

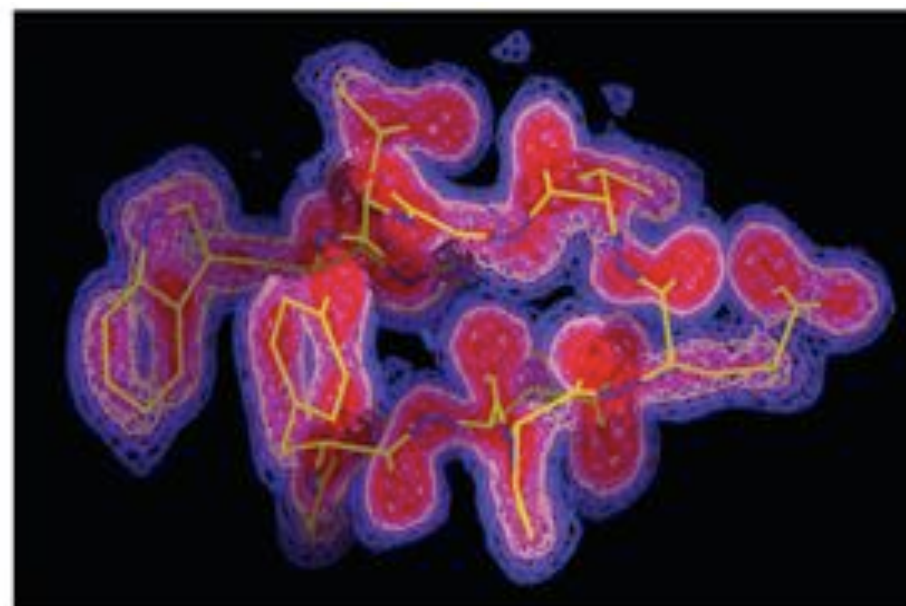
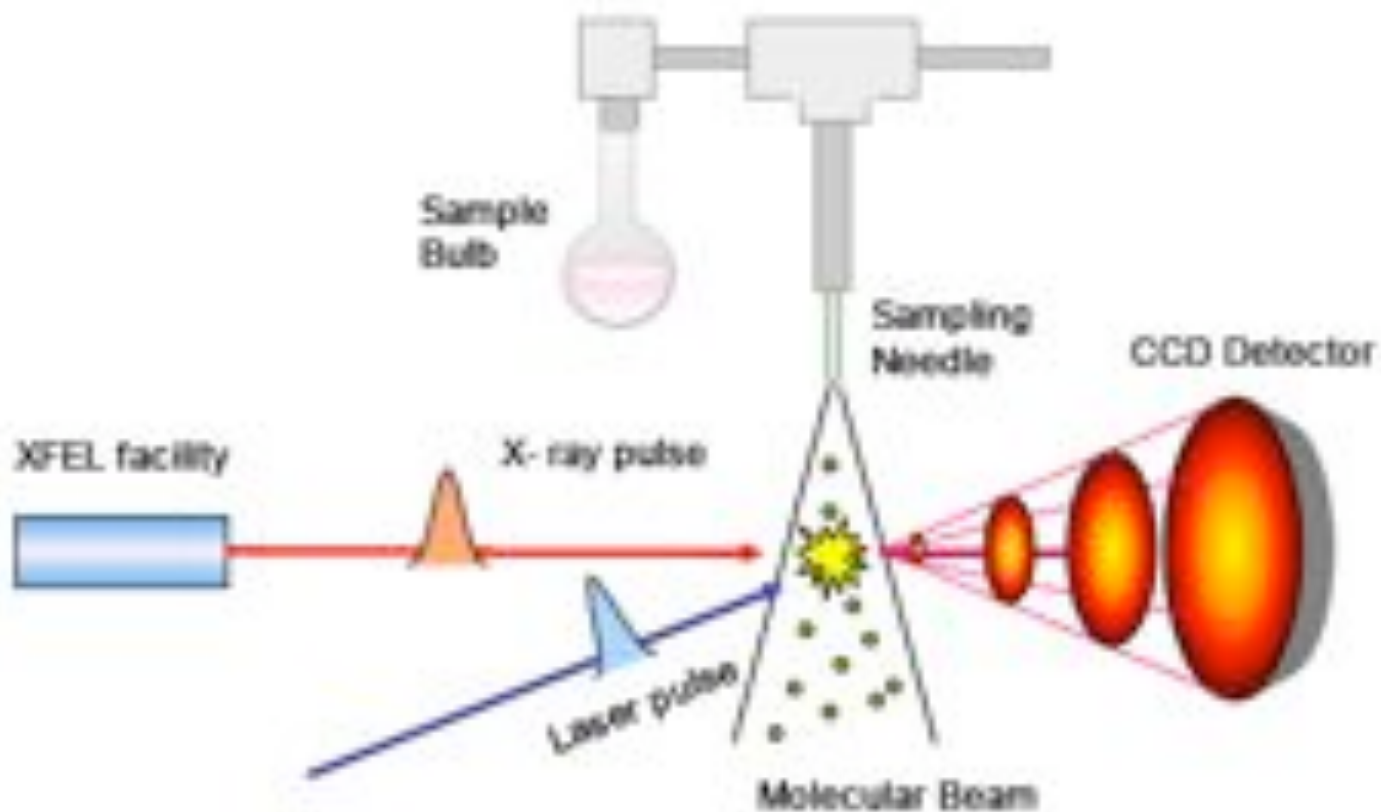
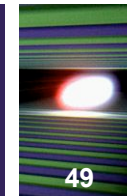
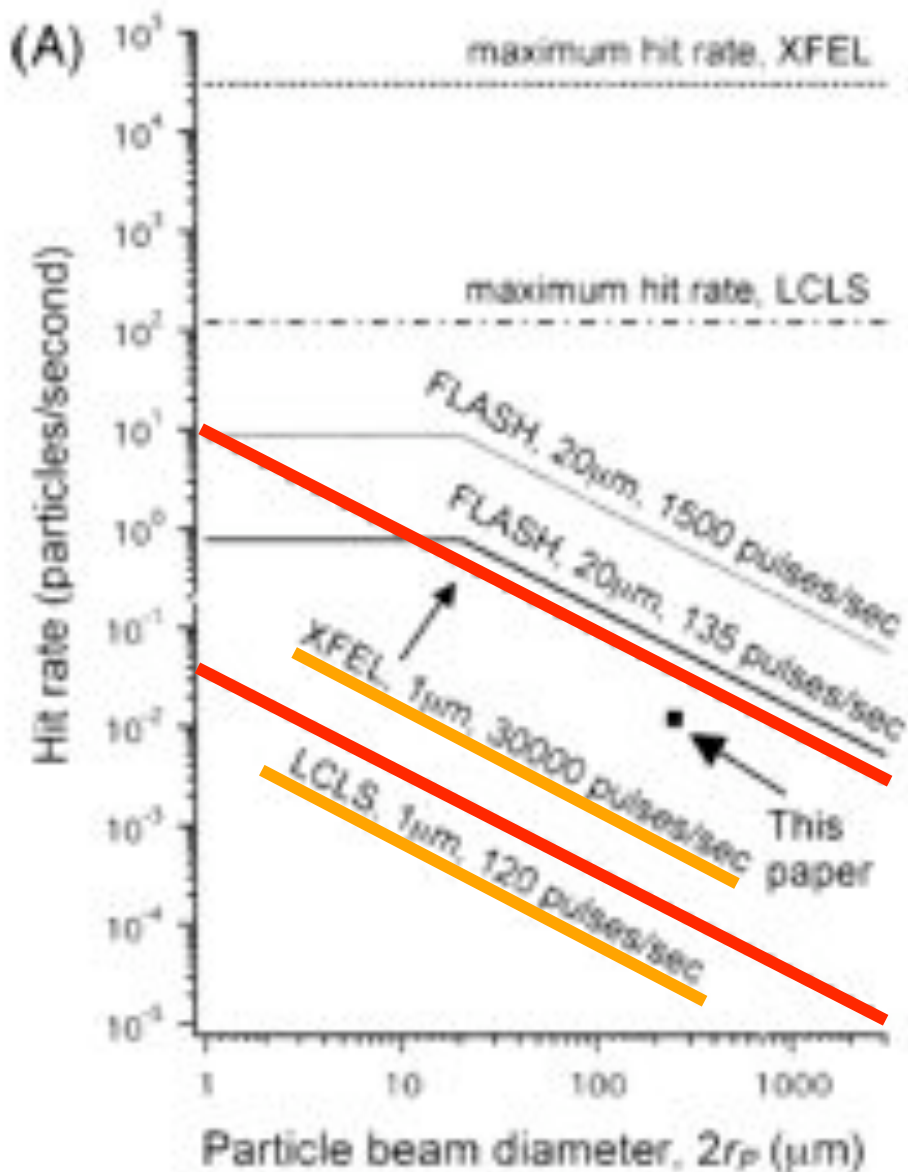
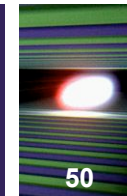


Figure 4 | Structure recovery. Isosurfaces of electron density of the protein chignolin, recovered from 72,000 diffraction patterns of unknown orientation at a MPC of 4×10^{-2} per pixel (see text). The molecular model is represented by the stick figure, with C bonds shown in yellow, N in blue and O in red. The 1, 2 and 3 σ electron density contours are shown in blue, pink and red, respectively, with σ denoting the r.m.s. deviation from the mean electron density.

Average Brilliance: Single-Particle Imaging





How many molecules are hit per second?

aerosol concentration of 3×10^4 particles/cm³

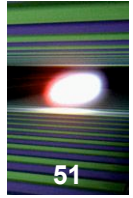
e.g.

FEL beam diam. 1 μm

Particle beam $\sim 200 \mu\text{m}$

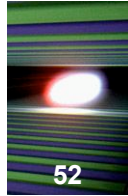
XFEL : ~ 0.1 hits per s

LCLS: $< 10^{-3}$ hits per s

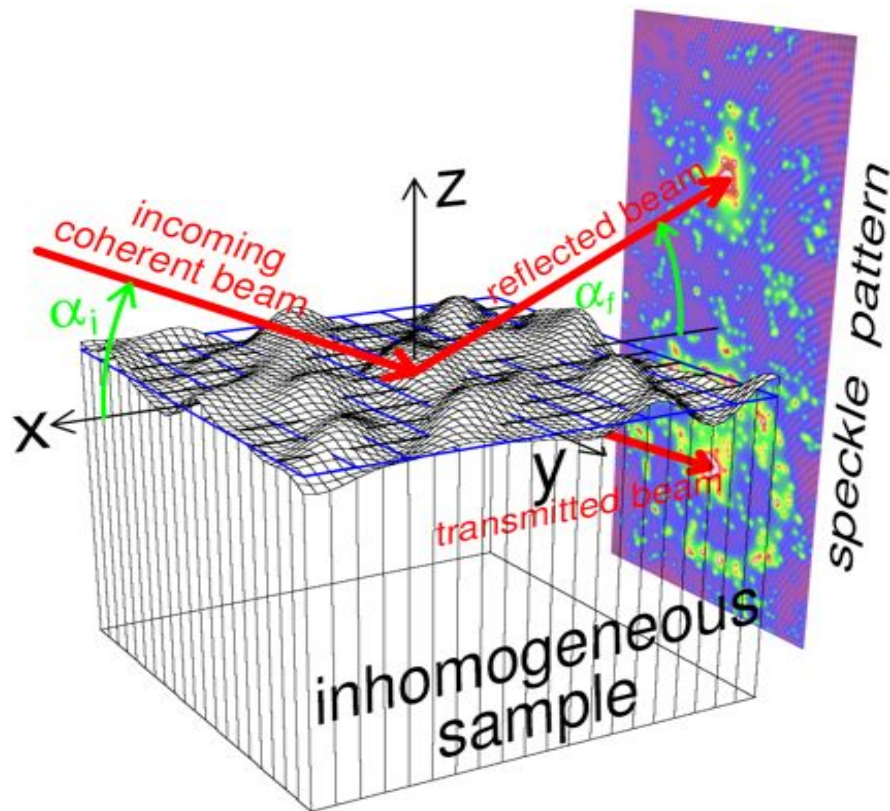


R&D projects of the European XFEL

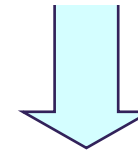
- Detectors allowing acquisition of images at 5 MHz
 - *3 Development projects under way for acquisition of up to 512 successive 1 M Pixel images at 5 MHz*
- Lasers allowing Pump and Probe at 5 MHz
 - *Plan launch of a development initiative in partnership with other institutes*



Coherent beam case: coherence length of light
at sample \gg correlation length of domains:



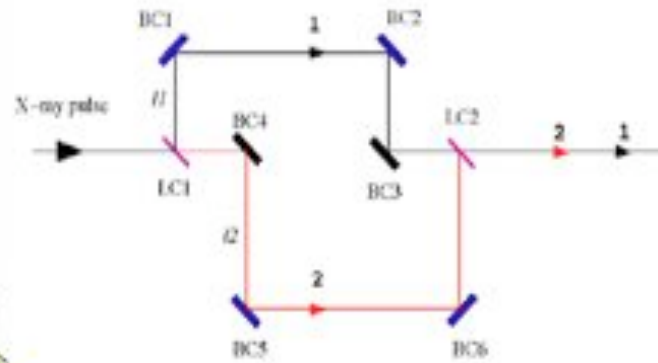
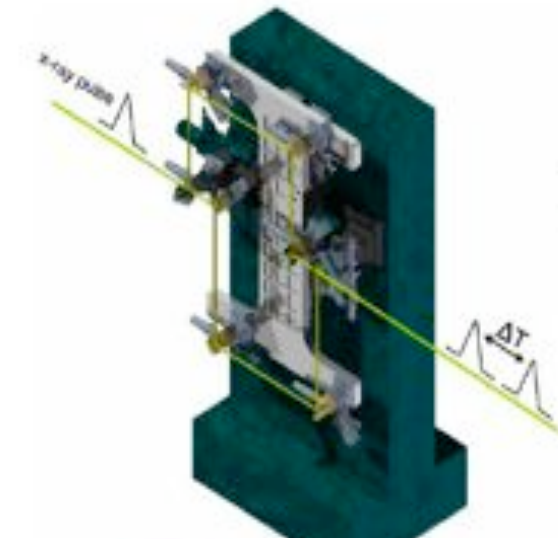
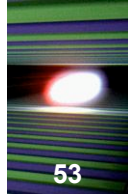
$$I(\mathbf{q}) = \left| \sum_{i=\text{domains}} e^{i\mathbf{q} \cdot \mathbf{R}_i} f_i \right|^2$$



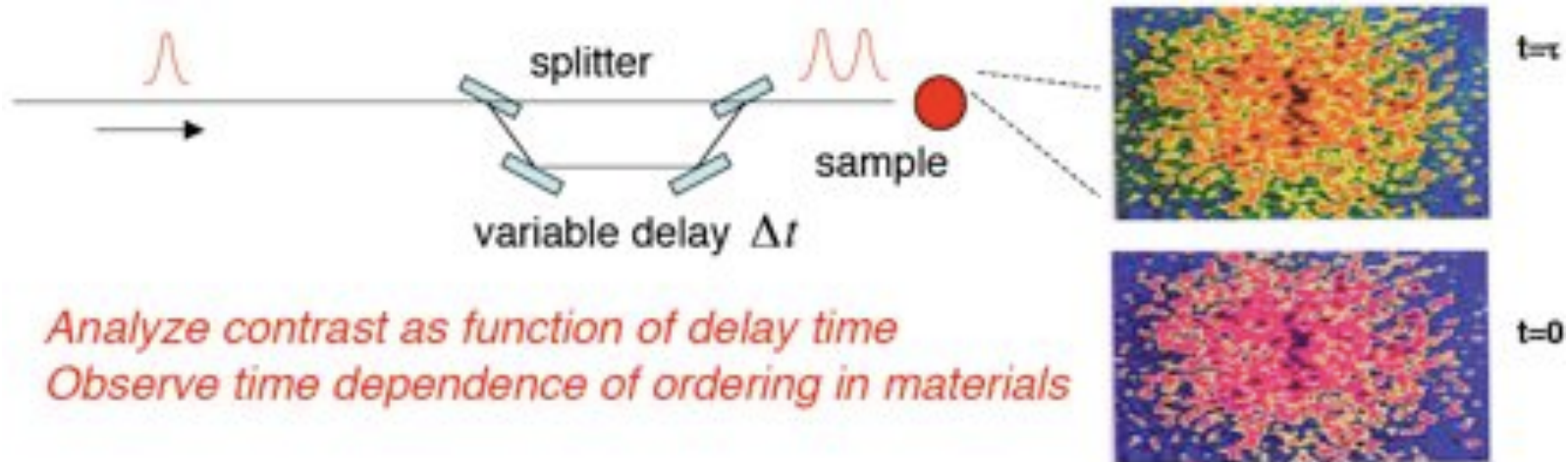
Fluctuating Intensity :

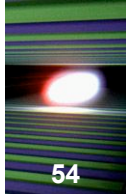
$$g_2(\tau) = \frac{\langle I(t+\tau)I(t) \rangle_t}{\langle I(t) \rangle_t^2}$$

Split-and-delay unit (Rosenker, Grübel *et al.*)

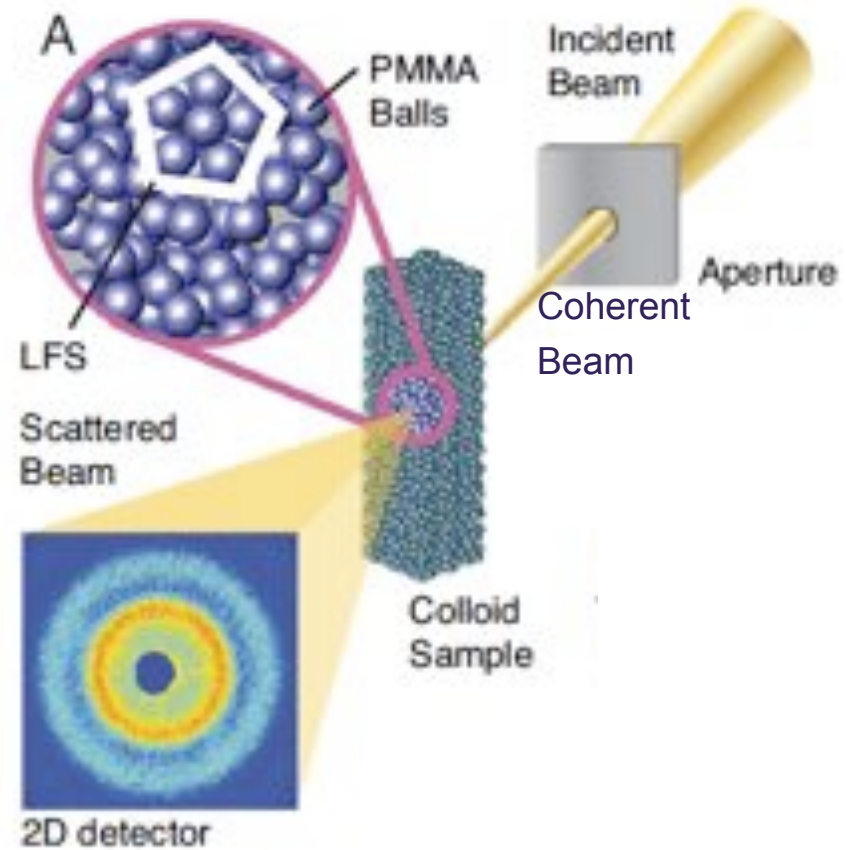
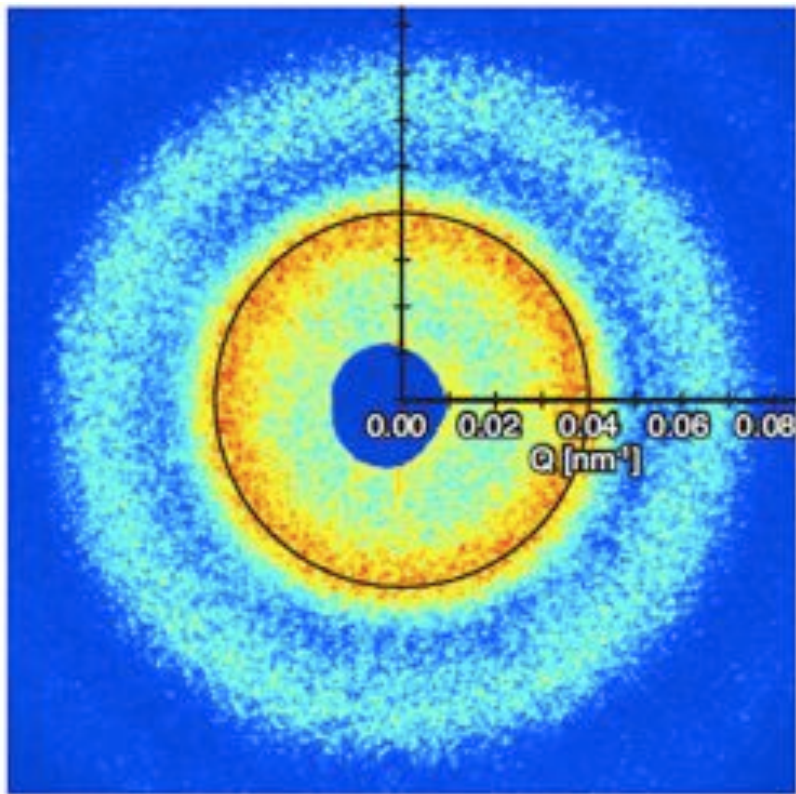


ps to ns delays



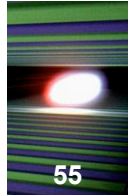


■ Speckle Scattering and Photon-Correlation Spectroscopy

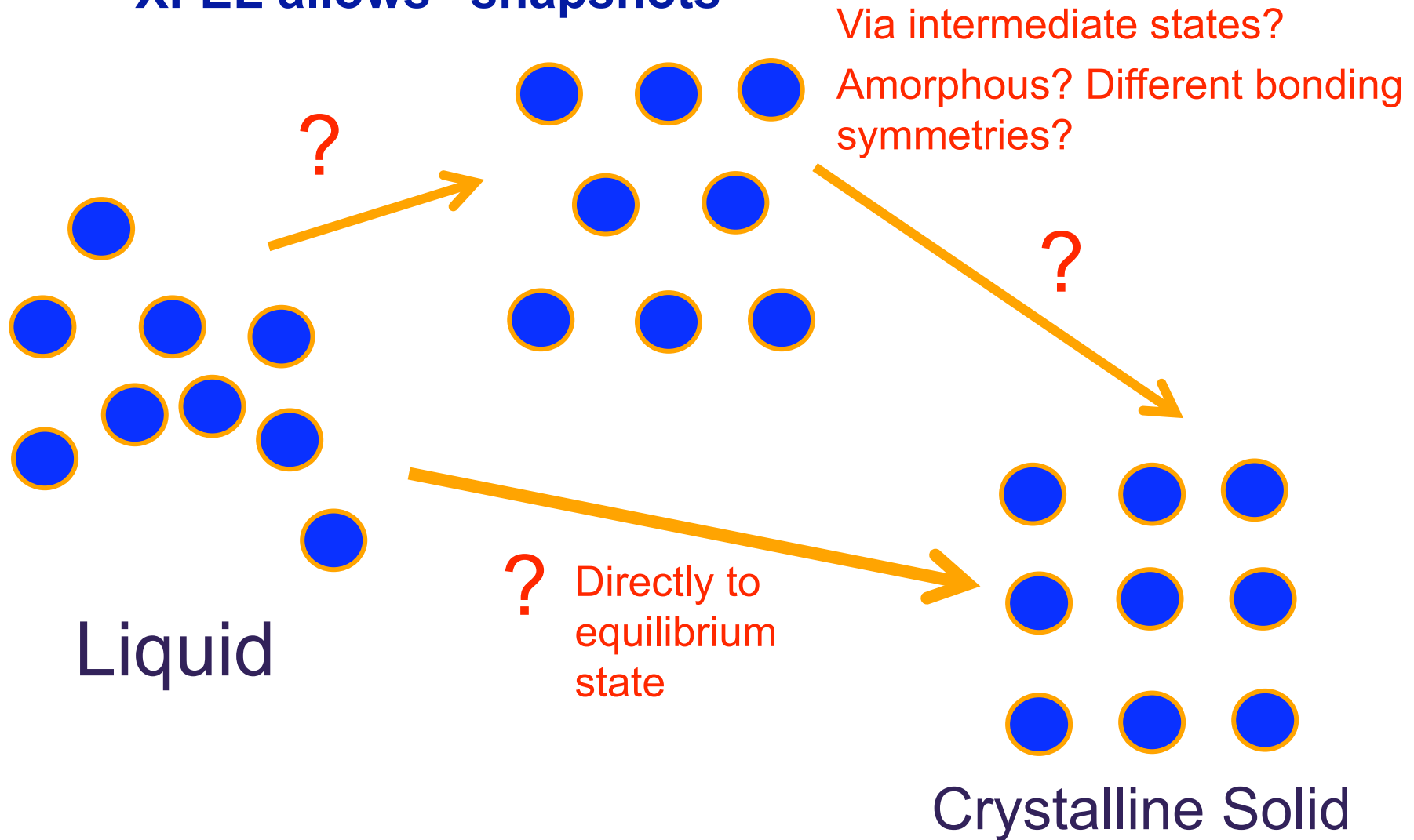


P. Wochner *et al.* PNAS (2009)

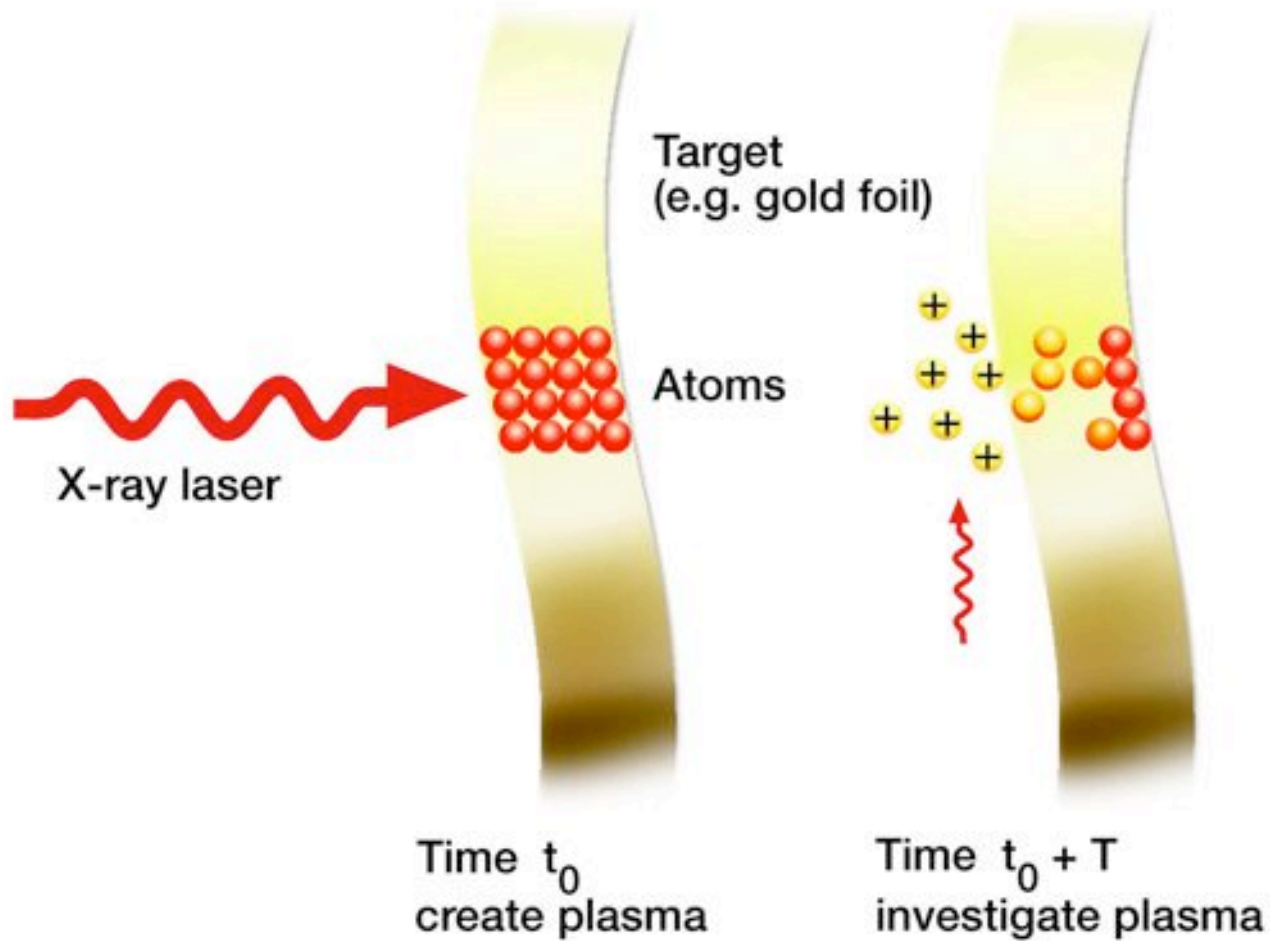
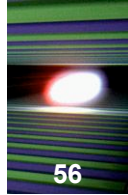
The formation of solid materials from liquids

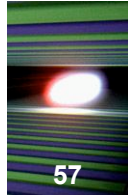


XFEL allows "snapshots"



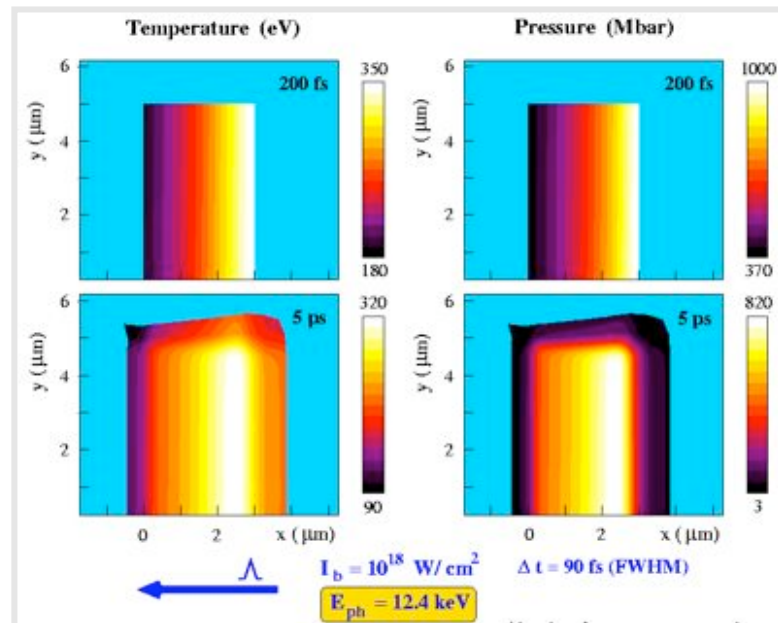
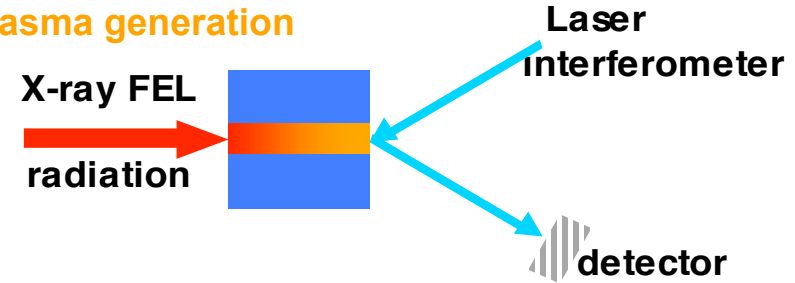
Plasma States by Pump-Probe Techniques



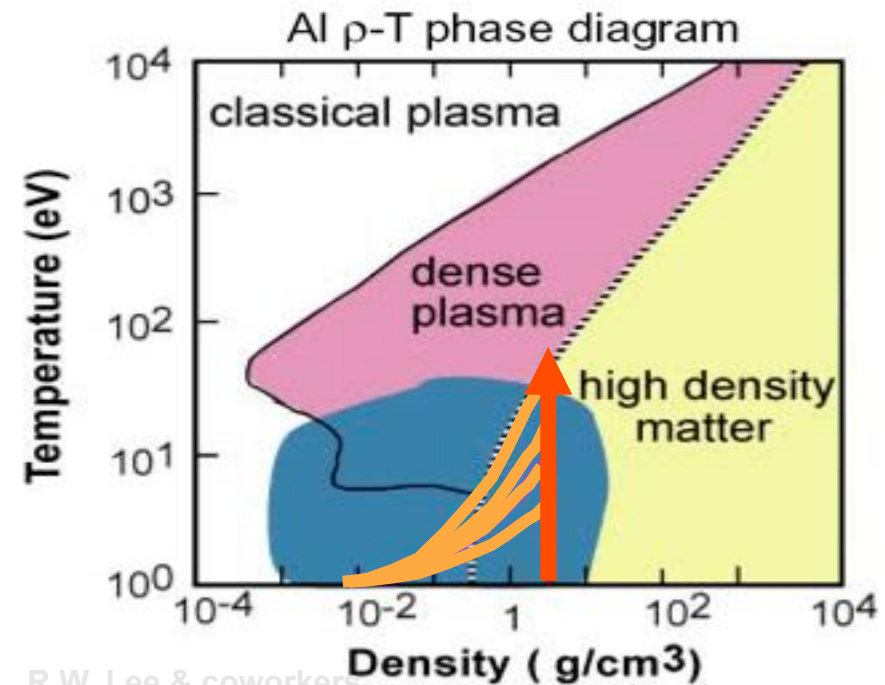


- Isochoric heating of plasmas
- Solid density plasmas
- T_e up to few 100 eV
- Warm dense matter
- Pressure up to Gbar
- Plasma phase transitions

Plasma generation



Schlegel et al., (2000)



R.W. Lee & coworkers

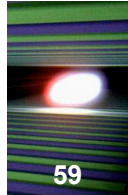
Int. Workshop on the High Energy Density Science Endstation and Associated Instrumentation at the European XFEL, Oxford, March 30 – April 1, 2009

Thomson scattering, warm dense matter, and interior of giant planets



Ronald Redmer
Universität Rostock
Institut für Physik
D-18051 Rostock
ronald.redmer@uni-rostock.de





Astrophysical objects

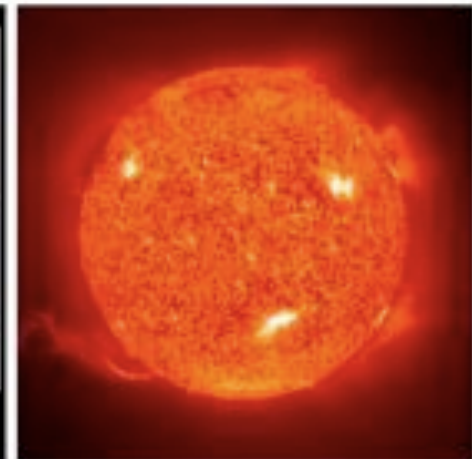
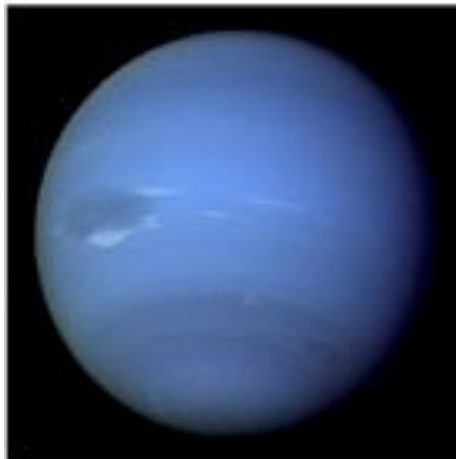
extreme states of matter

Ronald Redmer
Universität Rostock
Institut für Physik
D-18051 Rostock
ronald.redmer@uni-rostock.de

Giant Planets $M < 13M_J$

Brown Dwarfs $13M_J < M < 75M_J$

Stars $M > 75M_J$



J, S, U, N and more
than 300 exoplanets

... in the Orion Nebula
seen in the IR spectrum

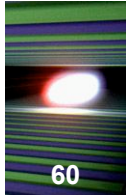
The Sun

Cores of GPs:
 $\approx 10^4$ K & 10 Mbar
warm dense matter

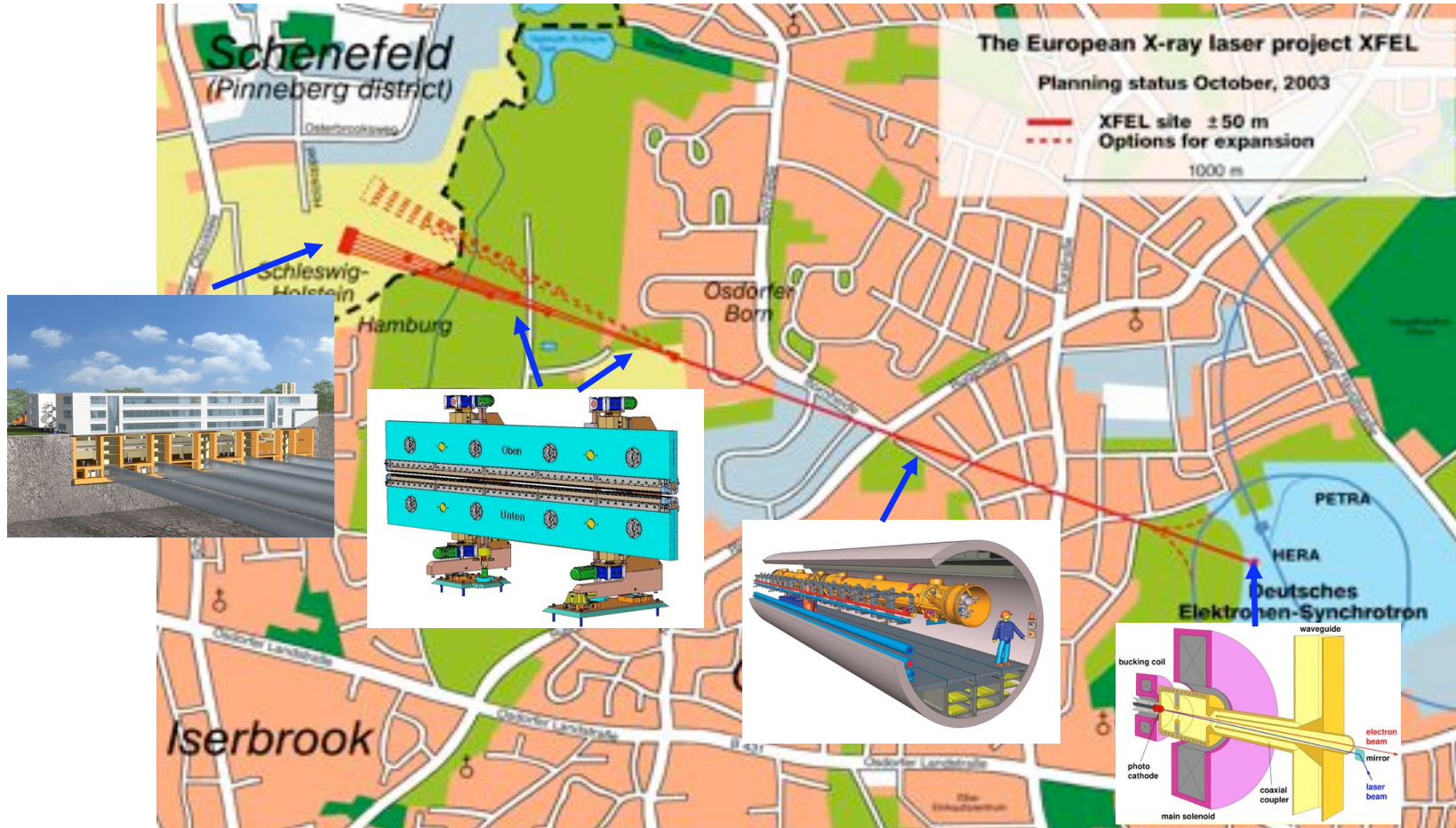
Cores of BDs:
 $\approx 10^6$ K & Gbar

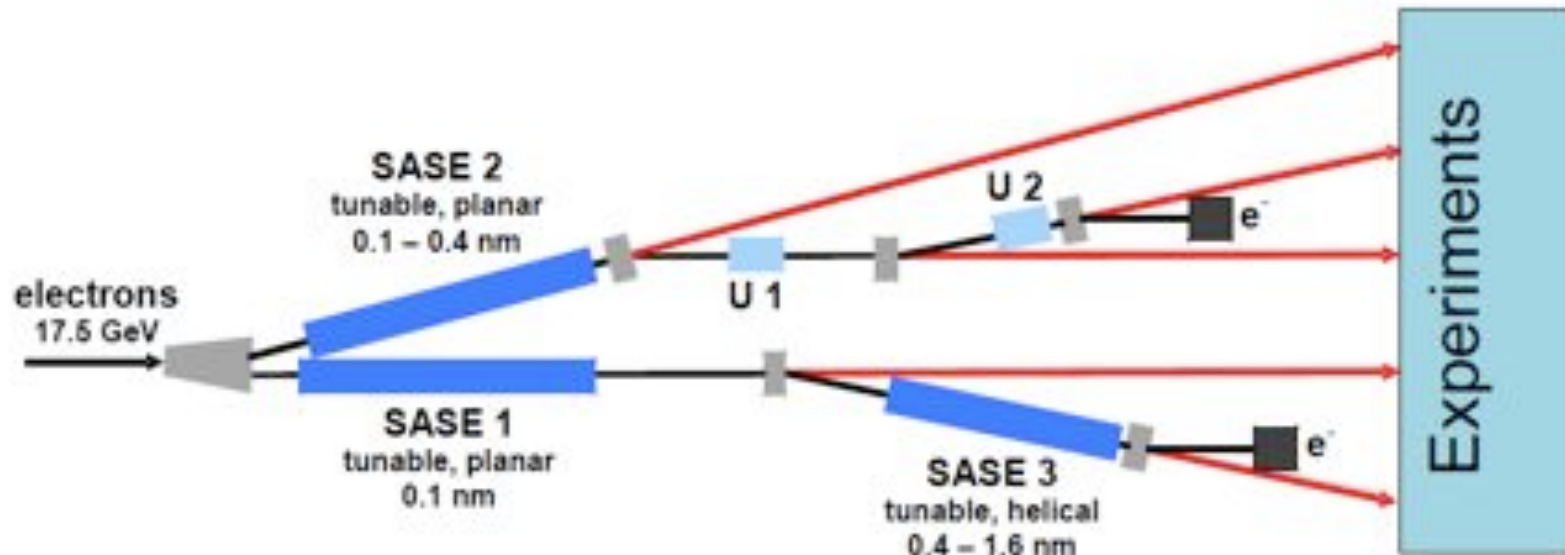
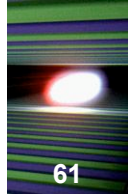
Core of the Sun:
 $\approx 10^7$ K & 100 Gbar
hot dense matter

Overall layout of the European XFEL



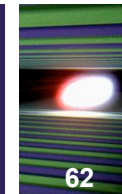
← 3.4km →



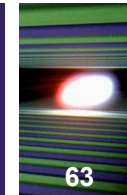


Initial configuration: SASE1, SASE2, SASE3 (planar)
plus six instruments

Photon Beam Parameters



Parameter	Unit	SASE 1	SASE 2		SASE 3		
Electron energy	GeV	17.5	17.5	17.5	17.5	17.5	10.0**
Wavelength	nm	0.1	0.1	0.4	0.4	1.6	6.4
Photon energy	keV	12.4	12.4	3.1	3.1	0.8	0.2
Peak power	GW	20	20	80	80	130	135
Average power*	W	65	65	260	260	420	580
Photon beam size (FWHM)	μm	70	85	55	60	70	95
Photon beam divergence (FWHM)	μrad	1	0.84	3.4	3.4	11.4	27
Coherence time	fs	0.2	0.22	0.38	0.34	0.88	1.9
Spectral bandwidth	%	0.08	0.08	0.18	0.2	0.3	0.73
Pulse duration	fs	100	100	100	100	100	100
Photons per pulse	#	10 ¹²	10 ¹²	1.6 × 10 ¹³	1.6 × 10 ¹³	1.0 × 10 ¹⁴	4.3 × 10 ¹⁴
Average flux	#/s	3.3 × 10 ¹⁶	3.3 × 10 ¹⁶	5.2 × 10 ¹⁷	5.2 × 10 ¹⁷	3.4 × 10 ¹⁸	1.4 × 10 ¹⁹
Peak brilliance	B	5.0 × 10 ³³	5.0 × 10 ³³	2.2 × 10 ³³	2.0 × 10 ³³	5.0 × 10 ³²	0.6 × 10 ³²
Average brilliance*	B	1.6 × 10 ²⁵	1.6 × 10 ²⁵	7.1 × 10 ²⁴	6.4 × 10 ²⁴	1.6 × 10 ²⁴	2.0 × 10 ²³



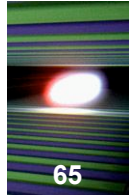
Instrument	Brief description of the instrument
SPB	Ultrafast Coherent Diffraction Imaging of Single Particles, Clusters, and Biomolecules – Structure determination of single particles: atomic clusters, bio-molecules, virus particles, cells.
MID	Materials Imaging & Dynamics – Structure determination of nano-devices and dynamics at the nanoscale.
FDE	Femtosecond Diffraction Experiments – Time-resolved investigations of the dynamics of solids, liquids, gases
HED	High Energy Density Matter – Investigation of matter under extreme conditions using hard x-rays, e.g. probing dense plasmas.
SQS	Small Quantum Systems – Investigation of atoms, ions, molecules and clusters in intense fields and non-linear phenomena.
SCS	Soft x-ray Coherent Scattering – Structure and dynamics of nano-systems and of non-reproducible biological objects using soft X-rays.

Hard X-rays

Soft X-rays



- Ensure exploitation of repetition rate at best
- Provide “simultaneous” beam time to different users’ groups
- Ensure high reliability and stability, top level experimental facilities



Thank you for your attention!

And thanks to my colleagues:

Reinhard Brinkmann

Serguei Molodtsov

Andreas Schwarz

Mikhail Yurkov